Increasing occupant localization precision through identification of footstep-contact dynamics

Slah Drira [a,b,*], Sai G.S. Pai [b], Ian F.C. Smith [a,b]

[a] *School of Architecture, Civil and Environmental Engineering (ENAC), Swiss Federal Institute of Technology (EPFL), Lausanne, Switzerland*
[b] *Future Cities Laboratory, Singapore-ETH Centre, Singapore*

ARTICLE INFO

ABSTRACT

Information regarding occupants inside buildings has the potential to improve security, energy management, and caregiving. Typical sensing approaches for occupant localization rely on mobile devices and cameras. These systems compromise privacy. Occupant localization using floor-vibration measurements, induced by footsteps, is a non-intrusive sensing method that requires few sensors (one per $\sim$35 m^2). Current occupant-localization methodologies that rely on vibration measurements are data-driven techniques. These techniques do not account for the structural behavior of floor slabs leading to ambiguous interpretations of vibrations measurement in the presence of obstructions and varying floor rigidities. In this paper, a model-based approach using error-domain model falsification (EDMF) is used to overcome these limitations. EDMF incorporates information related to physics-based models in the interpretation of vibration measurements to identify a population of possible occupant locations. EDMF accommodates systematic errors and model bias to reject models that contradict measurement data. Uncertainties from multiple sources such as modeling imperfection and walking-gait variability are included explicitly while estimating occupant locations using EDMF. A unique approach to identify footstep-contact dynamics is proposed and evaluated for its ability to improve the precision of occupant localization. The approach involves dividing the floor-slab into zones using knowledge of structural behavior. Clustering measured vibrations to define several footstep-contact severity levels helps reduce uncertainty in walking gait thus improving the accuracy of footstep-contact dynamics to use as loading input into model simulations. The utility of occupant localization using this approach is evaluated using a full-scale case study. Localization precision increased by more than 50% compared with non-zone-based strategies.

1. Introduction

Information regarding occupant locations inside buildings has the potential to improve important building functions such as security systems [1] and caregiving [2,3]. Moreover, understanding occupant flows inside buildings may be beneficial for space and energy management [4–7].

Current sensing technologies that have been used in occupant identification include cameras [8,9], and wearable devices such as smartphones [10,11]. However, optical sensors and radio-frequency devices typically required highly instrumented floors leading to regular maintenance [12–14]. Also, use of mobile devices and cameras are liable to privacy intrusiveness and inherently affected indoor occupant behavior. Alternative sensing approaches, such as acoustic devices [15,16], smart-flooring systems (pressure sensors) and vibration sensors [17] are

preferred since they preserved privacy. However, smart-flooring systems have required highly instrumented floors (thousands of sensors) [18,19]. Acoustic-based occupant localization have been compromised by ambient audible noise [20,21]. Such systems are not suitable for large full-scale applications. This study describes occupant localization using sparsely placed and non-intrusive sensors to measure floor vibrations that are induced by human footsteps.

Data-driven (non-physics-based or model-free) approaches, such as the time-difference-of-arrival (TDoA) method, have been carried out using footstep-induced vibration measurements for occupant localization [22–28]. TDoAs between measured footstep-induced floor vibrations at multiple sensors with overlapping coverage were used to triangulate occupant locations. Due to the dispersive nature of typical floor slabs, the wave propagation induced by footstep impacts resulted in low signal-to-noise ratio (SNR) vibrations, thereby leading to inaccurate localization. Thus, for full-scale applications, many sensors have

Nomenclature

Latin letters

$f_{i,j}$	Footstep-impact load model defining a contact-severity (S_j) level within a zone (Z_i)
f_c	Initial footstep-impact load model
f_{U_c}	Probability density function (PDF) of combined uncertainty
F1toF5	Force parameters that depend on body weight, contact-severity (S_j) level and zone (Z_i)
$g(\hat{A}\cdot)$	Function describing model prediction
m_e	Measured value of a footstep event
n_m	Number of measurement locations
Q	True structural response
S_i	Footstep-contact-severity level
$T_{high}; T_{low}$	Threshold bounds
T; T1 toT4	Time parameters that depend on contact-severity (S_j) level and zone (Z_i)
t	Time
U	Random variable of an observed error
$V_{i,j}$	Walking-gait variability defining a contact-severity (S_j) level within a zone (Z_i)
V_c	Initial walking-gait variability
W	Body weight
(x, y)	Occupant locations

Z_i	Zone of similar structural rigidity

Greek letters

Δ_{amp}	Maximum difference in amplitude of a footstep-impact signal
σ	Standard deviation of a footstep-impact signal
θ	Realization of model parameter to identify
ε	Error
ϕ	Target reliability of identification

Acronyms

CLS	Candidate-location set
CPSD	Cross-power spectral density
CWT	Continuous wavelet transform
EDMF	Error-domain model falsification
FDD	Frequency-domain decomposition approach
FHC	Full heel-contact
IHC	Initial heel-contact
IWT	Inverse wavelet transform
MS	Mid-stance phase
PDF	Probability density function
PS	Pre-swing phase
SNR	Signal-to-noise ratio
TDoA	Time-difference-of-arrival
TS	Terminal-stance phase
VGRF	Vertical-ground-reaction force

been required to provide accurate localization results (approximately one in 2 m^2) [29,30]. Even with many sensors, ambiguities are often unavoidable [31–33]. Supervised learning algorithms have also been employed for occupant localization using floor vibrations [34,35]. However, measurement scatter led to less than 60 % localization accuracy [34]. Xu et al [35] demonstrated that classification accuracy was sensitive to the walking speed. Localization accuracy did not exceed 70 % for occupants walking at a low-speed level.

Although model-free approaches may provide precise results for uniformly rigid floors (slabs on grade), more complex structural configurations (upper floors) and the presence of structural elements (such as beams and walls) have limited their applicability [25,29]. Floors supported by structural elements as well as the presence of non-structural elements result in changes in rigidity [36,37]. Varying floor-rigidity affects the wave propagation properties leading to inaccurate occupant localization using model-free approaches [25,34].

To date, the most common strategy has been to analyze signals from uniform rigidity floors in the absence of a structural behavior model. Aside from previous research by the current authors [31–33,37,38], no research has been found that involve simulations using physics-based models. These models help interpret floor-vibration measurements taken from sparse sensor configurations in order to localize occupants in terms of coordinates.

To overcome limitations of existing data-driven methodologies such as the TDoA technique, model-based data interpretation approaches have been proposed for occupant localization on upper floors [31–33]. A methodology that has been utilized for occupant localization is error-domain model falsification (EDMF) [39]. EDMF combines information related to measured footstep event signals with simulated physics-based models to identify a population of candidate occupant locations through eliminating locations that do not explain the measurements [31]. Occupant localization using EDMF accommodates biased uncertainties whose exact distributions are unknown. Incorporating systematic uncertainties and model bias, model falsification has provided accurate solutions for a range of inference tasks [40,41].

The precision of localization using EDMF depends upon the magnitude of uncertainties affecting falsification [31,37]. Typical uncertainty sources are measurements and most importantly, modeling assumptions. Footstep-induced floor vibrations are influenced by the natural variability in walking gait of the same person and between individuals [37]. Anatomies, walking speed, shoe type, health and mood affect the way occupants walk [42–44]. Variability in walking gaits has been evaluated for an occupant walking on the same footstep impact locations multiple times [31,37]. For several possible impact locations, relative measurement uncertainties were evaluated at more than 100%. In another study by the authors on a full-scale floor, walking-gait variability has been estimated for multiple occupants walking individually at the same locations, yielding a relative measurement uncertainty of ±45% [32].

Previous research by the authors into model-based occupant localization has involved finite element simulations of footstep impacts [31,32,37]. Simulations were affected by uncertainties from multiple sources [31–33]. Simplified finite-element modeling and an idealized footstep-impact load function used for simulation input resulted in systematic modelling uncertainties (bias). These uncertainties were taken to be uniform distributions between −65% to +25% in [31,33] and between −70% to +40% in [32]. Such high magnitudes of modelling uncertainties in EDMF has led to imprecise occupant localization [31–33]. Imprecise localization results restricted the usefulness of occupant-trajectory calculations. The aim of this study is to reduce the magnitude of uncertainties through a better estimation of walking-gait variability and a better definition of the footstep-load model in order to improve the accuracy of physics-based models.

The vertical ground reaction force (VGRF), defining the walking-gait pattern, has been modelled as an M-shaped force in the time domain [43]. This model involved three phases including heel phase, heel-to-toe phase and toe-off phase [43]. The heel phase was found to be the most important stage for the footstep impact regarding the floor response [43,45].

Describing an accurate footstep-impact load model requires the understanding of the contact dynamics transferred by individuals onto a floor slab. This description also needs an understanding of the floor

response generated by applied gait-pattern models [43,46]. Floor vibrations induced by footstep impacts depend on the relationship between natural bending modes and walking frequencies [46–48]. Civil-engineering structures have been divided into low-and-high frequency floors to characterize resonant and transient responses and thus, the design of the footstep-impact load model has been carried out separately for low-and-high frequency floors [46,49].

In the context of high-frequency floors (i.e. fundamental bending modes greater than 10 Hz [50]), footstep impacts produced a transient response [43,46,48]. Heel impacts had a dominant influence on the initial peak amplitudes followed by vibrations at bending modes of the floor slab. For each footstep impact, the resulting floor response presented a decaying rate related to the structural damping. Regarding the transient response, the dynamic load model for high-frequency floors was designed as an effective impulse as proposed by Willford et al. [46]. The resulting effective impulse values defined a decreasing trend when the natural frequency of the floor slab increased and the walking frequency decreased [46,47]. Thus, the proposed effective impulse accounted for the interaction between footstep impacts and structural characteristics.

However, the proposed effective impulse [46] does not account for the intra-subject variability [43,48]. The simulated vibration using the effective impulse results in similar vibrations for several footstep impacts compared with measured responses, which presented significant signal variabilities. Also, the proposed load model includes the assumption that the fundamental frequency of structure is constant [46]. This limits its applicability for varying-rigidity floors. Moreover, the artificial separation between structures is unreliable for floor slabs having significant responses in low-and-high frequency regions [48]. This results in the requirement for a more realistic dynamic model that accounts for complete frequency components of footstep-impact load forces.

Several studies have proposed definitions of the VGRF with the goal to be reliable for all floor slabs. For example, an idealized VGRF model was designed based on a sine function to model the heel and the toe-off phases and a plateau (defining the weight of an occupant) to model the heel-to-toe phase [51]. The range of values for each duration was determined based on a polynomial curve fit to footstep-induced floor vibrations. Moreover, the VGRF model was developed using sine functions to model the heel and the toe-off phases and a cosine function to model the heel-to-toe phase [52]. Load-parameter values (forces and durations defining each phase) were identified using a genetic algorithm on footstep-induced floor vibrations. However, the resulting parameter ranges were not valid for slow and moderate walking speeds. VGRF was also designed based on polynomial interpolation [53]. However, the proposed polynomial design was not able to include walking-gait variability since the heel-strike stage within the heel phase of the walking-gait pattern was omitted.

In this paper, occupant localization is studied using floor vibrations induced by footstep impacts that are detected by sparsely positioned sensors (approximately one in 35 m^2). Model-based data interpretation based on EDMF, which explicitly accommodates systematic uncertainty, is carried out for occupant localization. A novel footstep load model has been developed in this paper to serve as an input into occupant-localization simulations. This load model has been developed for various rigidities of floor slabs and VGRFs from multiple occupants. A new strategy for describing footstep-contact dynamics involving the understanding of structural behavior and footstep-induced floor vibrations is then presented. Finally, defining various levels of footstep-contact severity within zones of similar rigidities, a new zone-based occupant localization strategy is proposed.

The paper starts with a description of the occupant detection and localization framework (Section 2). Mathematical and physical details of the data interpretation methodology for occupant localization (EDMF) is presented in Section 3.1. Design of footstep-impact load function and walking-gait variability are explained in Sections 3.2 and

3.3. The footstep-contact-dynamics identification strategy is described in Section 3.4. The zone-based occupant-localization strategy is then presented in Section 3.5. A full-scale case-study description for occupant localization is given in Section 4. Subsequently, an application of the zone-based occupant-localization strategy on full-scale floor slab illustrates the method in Section 5.

2. Occupant detection-and-tracking framework

In this framework, footstep-event signals are used to detect occupants and then infer possible locations as an inverse problem on complex full-scale slabs (upper floors). The resulting locations are then used to ascertain possible walking trajectories of occupants.

Vibration measurements are regularly contaminated by several activity sources including door closing, falling objects and electrical devices (such as a fan). Moreover, floor-vibration magnitudes are governed by structural behavior and influenced by obstructions such as beams and walls. Also, gaits of occupants walking along similar trajectories vary due to their anatomies, speed levels, type of shoes, health, mood etc. This leads to significant variability in footstep-event signals. These uncertainties lead to ambiguities in the interpretation of floor vibrations, thereby, making occupant detection and tracking a challenging task. The novelty of the proposed framework is that information on structural behavior and various uncertainty sources are combined to achieve accurate and precise detection and tracking of occupants.

Steps that are involved in this framework are shown in Fig. 1. The framework starts with a model-free occupant detection operation. This operation involves extracting event signals and then identifying signals that correspond to footstep events using supervised learning techniques, as presented by Drira et al. [54].

Subsequently, a zone-based occupant localization approach, which is the focus of this paper, is carried out to identify probable positions of individual occupants, as shown in Fig. 1. Details of the zone-based occupant localization approach is described in Section 3. This novel occupant-localization methodology includes a model-based data interpretation approach that combines information from measured footstep-event signals with physics-based models [31–33,36] (see Section 3).
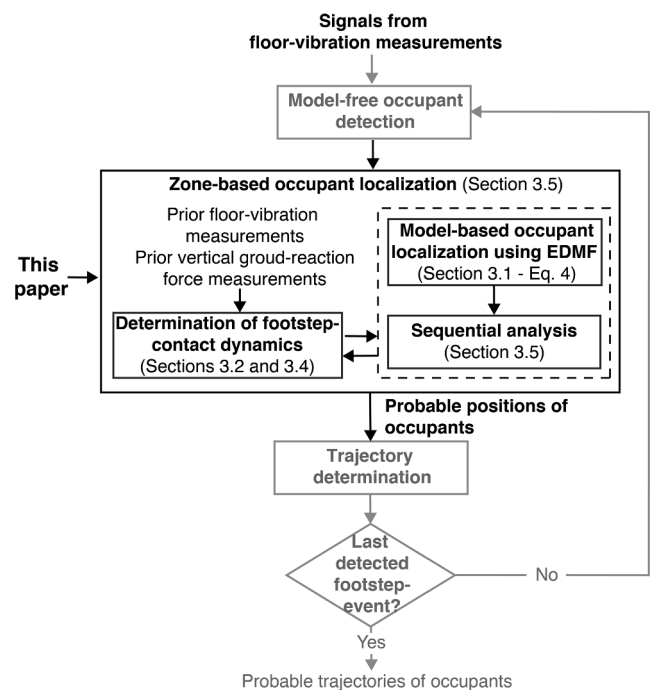

Fig. 1. Framework for occupant detection and tracking. Relevant section numbers in this paper are noted.

Error-domain model-falsification (EDMF) [39] is a model-based data interpretation approach that has already been applied by the authors to identify a population of possible locations of occupants [31].

Within the scope of this paper, a new strategy that combines a sequential analysis and information of footstep-contact dynamics is proposed to enhance the localization results obtained from the falsification process (see Section 3). The sequential analysis accommodates information from the previously detected footsteps to enhance the precision of occupant location for the current footstep event. The determination of footstep-contact dynamics (see Section 3) involves decomposing the floor-slab into zones using knowledge of structural behavior to reduce variability in walking gaits.

Localization results of each detected event are used to determine possible trajectories. As noted in Fig. 1, the trajectory-determination operation is beyond the scope of this paper. Details of the trajectory-determination strategy are presented by Drira et al [32]. These operations are repeated for each measured footstep event.

3. Occupant localization

3.1. Background - Error-domain model falsification

Error-domain model falsification (EDMF) is a model-based data-interpretation approach that was proposed by Goulet and Smith [39]. EDMF involves simulation of a population of initial model instances (i.e. physics-based model instances) of a system to interpret measurement data [55]. The initial model instances are simulated using possible ranges of primary parameter values that are estimated based on prior information about a system and engineering knowledge. Predictions from these models are then compared with the measured structural response to identify candidate models amongst the initial population. Initial model instances that are not falsified form a candidate-model set. This is compatible with a well-established scientific viewpoint that measurement data are more useful when they falsify (refute) models (strong science) compared with using measurement data to validate models (weak science) [56].

In the context of model falsification, the predicted response at measurement location l is denoted as $g_l(\theta)$ in which θ corresponds to the model parameter values to be identified, which in this case, are the occupant locations (x, y). The measured response at sensor location l is denoted as m_l.

Modelling and measurement uncertainties associated with each measurement location are $\varepsilon_{mod,l}$ and $\varepsilon_{meas,l}$ respectively. Modelling uncertainties result from conservative and simplified models. These uncertainties are intrinsically systematic. Measurement uncertainties define the variability in measured responses. For model-based occupant localization, the natural variability in walking gaits contributes the most to uncertainty in measured floor vibrations. Quantification of these uncertainties is based on engineering judgment and prior observations [31,57].

The unknown true structural response at a measurement location i is denoted as Q_l, as shown in Eq. (1) where n_m is the total number of measurement locations. The true structural response, Q_l, equals either the sum of model prediction for parameters of the position vector θ, $g_l(\theta^*)$, with true (*) parameter values, θ^*, conditioned by modelling error, $\varepsilon_{mod,l}$, or the sum of measured response, m_l, conditioned by measurement error, $\varepsilon_{meas,l}$.

$$Q_l = g_l(\theta^*) + \varepsilon_{mod,l} = m_l + \varepsilon_{meas,l} \forall l \in \{1,..,n_m\} \tag{1}$$

Rearranging Eq. (1), the residual between the predicted and measured responses is equal to the combined uncertainty, $\varepsilon_{c,l}$, at a measurement location l as shown in Eq. (2).

$$g_l(\theta^*) - m_l = \varepsilon_{meas,l} - \varepsilon_{mod,l} = \varepsilon_{c,l} \tag{2}$$

In a probabilistic approach, modelling, measurement and combined

uncertainties are random variables denoted as $U_{mod,l}$, $U_{meas,l}$, $U_{c,l}$ of observed errors $\varepsilon_{mod,l}$, $\varepsilon_{meas,l}$, $\varepsilon_{c,l}$ respectively. Generally, due to the lack of information of the uncertainty distributions, these uncertainties are assumed to follow a uniform distribution. Uniform distributions have the advantage that correlations between variables do not need to be quantified [58]. There is no requirement for zero-mean distributions. Thus, uncertainties, particularly $U_{mod,l}$ can be transparently represented with a bias.

Measurement and modelling uncertainties are combined using Monte Carlo sampling. The combined uncertainty ($U_{c,l}$) and a target reliability of identification (ϕ) are used to compute the identification thresholds ($T_{high,l}$ and $T_{low,l}$), Eq. (3) [39,59]. These thresholds are defined to be the shortest distance that satisfies Eq. (3) for the combined uncertainty distribution. The typical value of target reliability of identification, ϕ, in structural engineering is equal to 0.95.

$$\phi^{1/n_m} = \int_{T_{low,l}}^{T_{high,l}} f_{U_{c,l}}(U_{c,l}) dU_{c,l} \phi \in \{0,1\} \tag{3}$$

In Eq. (3), $f_{U_{c,l}}$ is the probability density function (PDF) of the combined uncertainty, $U_{c,l}$. The term $1/n_m$, in Eq. (3), is the Šidák correction [60] that is applied to ensure that the reliability of identification remains constant with increasing number of measurements, n_m.

For occupant-localization applications, as described by Drira et al. [31], a schematic representation of model-based localization using EDMF is shown in Fig. 2. Model parameter values, θ, represents couples of x and y coordinates of possible occupant locations on the floor slab, as presented by dots in Fig. 2. Footstep-impact simulations are $g_l(\theta)$ and floor-vibration measurement induced by a detected footstep event (e) is $m_{l,e}$, see Eq. (4).

$$T_{low,l,e} \leq g_l(\theta) - m_{l,e} \leq T_{high,l,e} \forall l \in \{1,..,n_m\} \tag{4}$$

Model predictions at possible locations ($g_l(\theta)$) are typically obtained using finite element models. While building drawings are generally available to carry out the finite element models for simulations, in-situ inspection is essential to verify the as-built geometry.

The distribution shown in Fig. 2 defines a schematic representation of the PDF of combined uncertainty. As shown in Fig. 2, for each detected footstep event (e), model predictions defining all location instances whose residuals with a measured footstep event lie inside the localization thresholds ($T_{low,l,e}$ and $T_{high,l,e}$) at each sensor location (l) are accepted and thus form the candidate-location set (CLS) satisfying Eq. (4) [31–33,38]. This operation is repeated for each detected footstep event (see Fig. 1).

The identification of position vector θ (x and y coordinates) of occupants is not computationally expensive since measured footstep-event signal is compared with pre-simulated footstep impacts at a grid of possible locations. These simulations allow repeated use of the same simulation results for multiple comparisons with all measured footstep-event signals. Thus, model falsification allows a near-real-time localization of occupant footsteps. EDMF provides a population of possible locations and all candidate models are assumed to be equally probable due to the lack of information of true uncertainty distributions. Finally, since EDMF is a constrained satisfaction procedure, there are no difficulties with convergence as there may be with conventional optimization methods.

3.2. Footstep-impact load model for simulation input

For model-based occupant localization, footstep-impact simulations are performed using an input load model that reflects the walking-gait cycle in the time domain. The load model is constructed using sine and cosine functions (see Fig. 3 and Eq. (5)). The vertical force pattern resulting from a walking-gait cycle is composed of three phases: heel phase heel-to-toe phase and toe-off phase [43]. Measured VGRF induced
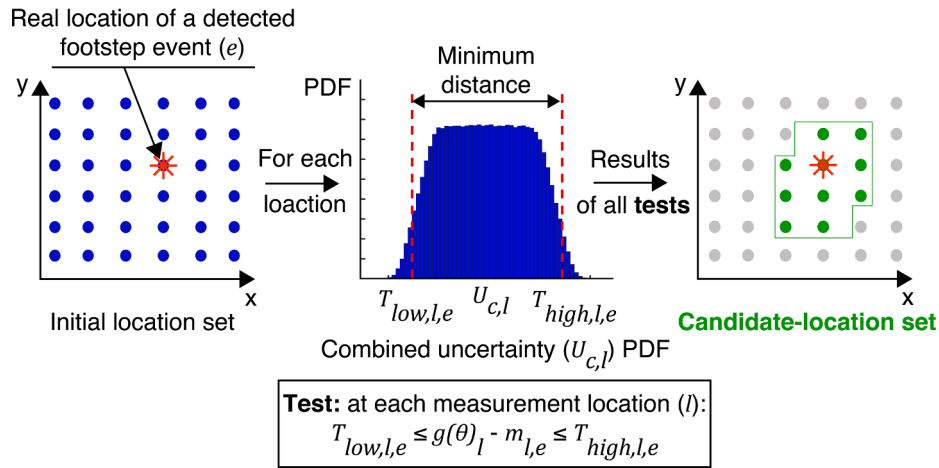
Fig. 2. Location identification using error-domain model-falsification starts with an initial location set. Model simulations are compared with measured response in order to identify candidate locations among the initial population. Threshold boundaries are derived from the PDF of the combined uncertainties. Model instances are falsified when the residual value between simulations and measurements exceeds thresholds at any sensor location.
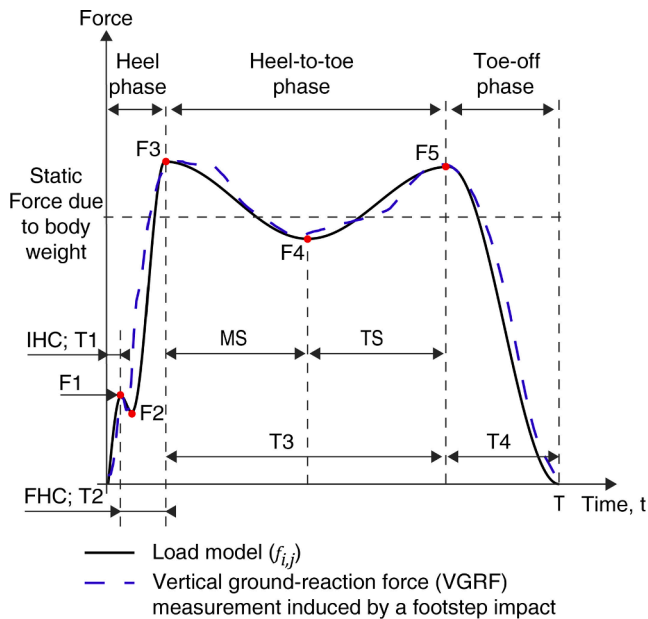

Fig. 3. Measured vertical ground-reaction force (VGRF) induced by a footstep impact compared with a load model. The load model is constructed using sine and cosine functions (see Eq. (5)). VGRF measurements are recorded using a pressure plate mounted on the ground.

by a footstep impact compared with the proposed load model in the time domain is illustrated in Fig. 3.

In Fig. 3, the heel phase begins with an initial heel-contact (IHC) phase and ends with a full heel-contact (FHC) phase. IHC phase refers to a brief duration (T1) when the heel part of the foot first hits the floor. F1 refers to the abrupt transfer of body weight to the floor slab. The attenuation of the IHC force refers to a reaction force F2. FHC phase refers to the duration (T2), during which the foot is in full contact with the floor surface. The FHC phase ends when the VGRF reaches a maximum (F3).

Subsequent to full contact of the heel with the floor, the heel-to-toe

phase begins. The duration of the heel-to-toe phase is defined as T3. This phase begins with a period of mid-stance (MS). During this period, the body weight is supported by the stance limb, while the opposite foot starts to leave the floor surface for the next footstep impact. The vertical force, during the MS period, reaches a minimum (F4) once the heel of the stance limb starts to rise from the floor surface (i.e. heel off). The MS period is succeeded with a terminal stance period (TS). The TS period begins with a heel off, thereby the foot contact is transferred to toes. During the TS period, the vertical force trend ascends to a maximum (F5) until the other foot strikes the floor.

Finally, rising of the stance limb (toe-off) from the ground refers to the toe-off phase. The duration of the toe-off phase is defined as T4 in Fig. 3. During this phase, the vertical force descends to zero defining the overall duration of the footstep impact, denoted as T. The toe-off phase is also defined as a pre-swing phase (PS). During the PS phase, the stance limb swings for the next footstep event.

The load model ($f_{i,j}$), function of time (t), is composed of four sine functions and a cosine function, as shown in Eq. (5). Forces F1 to F5, body weight (W) and durations T1 to T4 and T are parameters of the load model (see Fig. 3). The indexes, i and j, which are defined in Section 3.4 determine the unique value for force and time parameters. The first part of the load model, represented as a sine function (see Eq. (5)), defines the IHC phase. The second part of the load model, also represented as a sine function (see Eq. (5)), models the attenuation of the IHC force. The duration of the second part is assumed to be equal to the quarter of the initial-to-full heel contact duration (T2). This estimate is based on prior analysis of VGRF measurements from multiple occupants [61].

The third part of the load model, also a sine function, is the FHC phase. The sine function is used to link the forces F2 and F3. The fourth part of the load function that defines to the heel-to-toe phase is represented by a cosine function. This part contains a linear function that is used to link the forces F3 and F5. For this part, the duration of the MS and TS phases are assumed to be equal. The final part of the load model that models the toe-off phase is modelled using a sine function. T is the footstep-impact duration. Including several forces and durations (forces F1 to F5 and durations T1 to T4 and T in Fig. 3) as parameters of the load model (see Eq. (5)), helps assess variability in walking gaits, which is discussed next in Section 3.3.

$$f_{i,j} = \begin{cases} F1\sin\left(\frac{2\pi t}{T1}\right) & \text{if} \quad t \in [0..T1]s \\ F2 + \frac{F1 - F2}{2}\left(1 + \sin\left(-\frac{4\pi}{T2}\left(t - T1 + \frac{3T2}{8}\right)\right)\right) & \text{if} \quad t \in \left[T1..T1 + \frac{T2}{4}\right]s \\ F2 + \frac{F3 - F2}{2}\left(1 + \sin\left(\frac{4\pi}{3T2}\left(t - T1 + \frac{7T2}{8}\right)\right)\right) & \text{if} \quad t \in \left[T1 + \frac{T2}{4}..T1 + T2\right]s \\ F4 + \frac{F3 - F4}{2}\left(1 + \cos\left(\frac{2\pi}{T3}(t - T1 - T2)\right)\right) + (t - T1 - T2)\frac{F5 - F3}{T3} & \text{if} \quad t \in [T1 + T2..T - T4]s \\ \frac{F5}{2}\left(1 + \sin\left(-\frac{\pi}{T3}\left(t - \frac{5}{2}(T - T4)\right)\right)\right) & \text{if} \quad t \in [T - T4..T]s \end{cases} \tag{5}$$

3.3. Sources of variability in walking gait

Values of parameter ranges of the load model (see Eq. (5)) are determined using VGRF measurements induced by footstep impacts (see Fig. 3). These parameters are body weights, forces F1 to F5 and durations T1 to T3, as shown in Fig. 3. Walking styles differ among occupants due to their anatomies, walking speed, shoe type, health and mood. Thus, determining parameter ranges of the proposed load model helps understand the variability in walking gaits.

483 measurements of footstep induced VGRFs have been carried out. These measurements have been recorded for 12 healthy occupants walking at no-fixed speed. Measurements have been recorded using a pressure plate mounted on the ground with a sampling rate of 200 Hz. Occupant weights vary between 63 and 82 Kg and their heights vary between 165 and 186 cm. These measurements have been carried out at the Laboratory of Movement Analysis and Measurement (EPFL, Switzerland) [61].

The minimum and the maximum bounds of each parameter, resulting from VGRF measurements, are presented in Table 1. Bounds are determined based on 95th percentile of each parameter distribution. Forces F1, F3, and F5 are proportional to bodyweights. Forces F2 and F4 are proportional to the forces F1 and F3 respectively. The resulting parameter ranges are extended by up to 10% to account for variability in walking gait outside the bounds of experimental evaluation.

3.4. Footstep-contact dynamics for precise simulation input

Prior to the localization process using the zone-based localization approach (Section 3.5), the determination of footstep-contact dynamics is carried out. The information of footstep-contact dynamics is used to enhance model predictions and improve estimation of walking gait variability. This improves localization precision, which evaluated in

Table 1

. The load model (see Eq. (5)) parameter value ranges that are determined using measurements of VGRF induced by footstep impacts. Value ranges are extended to assess greater variability for footstep-impact simulations.

	Footstep-load function parameter	Parameter value range	Extended range
W	Body weight (Kg)	[63–82]	[60–90]
F1	Initial heel-contact force (Kg)	[0.25–0.52] × W	[0.2–0.6] × W
F2	Initial-to-full heel-contact force (Kg)	[0.61–0.94] × F1	[0.6–0.9] × F1
F3	Full heel-contact force (Kg)	[1.1–1.5] × W	[1.0–1.5] × W
F4	Heel-to-toe contact force (Kg)	[0.5–0.83] × F3	[0.5–0.9] × F3
F5	Toe contact force (Kg)	[1–1.3] × W	[1–1.3] × W
T1	Initial heel-contact duration (s)	[0.01–0.04]	[0.01–0.04]
T2	Full heel-contact duration (s)	[0.04–0.2]	[0.04–0.2]
T3	Heel-to-toe contact duration (s)	[0.34–0.58]	[0.3–0.6]
T	Footstep-impact duration (s)	[0.7–0.9]	[0.7–0.9]

Section 5.

Occupant footstep contact-severity levels are classified as low, medium and hard using footstep-induced floor vibrations. The determination of footstep-contact dynamics involves assessing the variability in load for each contact-severity level using measured vibrations. Load functions (see Eq. (5)) designed for each contact-severity level are used to simulate footstep impacts at possible locations on a floor for model-based occupant localization (see Section 3.2).

Typical floor-slabs are obstructed by structural and non-structural elements such as walls, beams and columns. These obstructions change the rigidity of the floor. Varying floor-rigidity affects wave propagation properties leading to variability in structural responses induced by footstep impacts [36,62]. Thus, the floor area is divided into zones (Z_i) that have similar structural rigidities, where the index, i, is the zone number. The load model ($f_{i,j}$) and the walking-gait variability ($V_{i,j}$) are ascertained for each contact-severity (S_j) level in each Z_i. The index, j, represents the level of contact severity (low, medium and hard). The relevant steps involved in the determination of footstep-contact dynamics are outlined in Fig. 4.

Zones of similar vertical rigidities are determined though modal analysis of the floor slab using ambient vibration measurements. Vertical mode-shapes, corresponding to fundamental bending modes of the floor slab, are found using frequency-domain decomposition (FDD) [63]. A sensor configuration covering the entire space of a floor is used to measure ambient vibrations. This helps provide good estimates of bending mode shapes resulting from the FDD approach. FDD involves computing the cross-power spectral density (CPSD) [64] of ambient vibrations recorded by each sensor configuration. CPSD matrices are then decomposed into singular values and vectors.

The singular values of the CPSD matrices define the fundamental frequencies of the floor slab. Their corresponding singular vectors are estimates of mode shapes. Typically, prominent peaks resulting from singular-value decomposition are the first few modes of the floor slab. A zone (Z_i) defines an area on the floor that represents regions with similar deflections when first and second mode shapes of the slab are excited. Coordinates of the centroid for each predefined Z_i are subsequently involved in the zone-based occupant localization approach (see Section 3.5).

Floor vibrations from multiple people walking with various speed levels at fixed locations and wearing different types of shoes are used to define groups of similar vibration magnitudes. Footstep-event signals belonging to each zone (Z_i) are clustered using the k-means algorithm [65]. K-means clustering is a well-established unsupervised learning method that typically employs spatial metrics such as the Euclidean distance to assess the similarity between entities. The number of groups (k) has to be defined before clustering. Three clusters are provided as input to define low, medium and hard contact-severity levels ($S_{j=1..3}$). K-means clustering results in decision boundaries (for each S_j level in each Z_i) that help assign future footstep-event signals to their respective
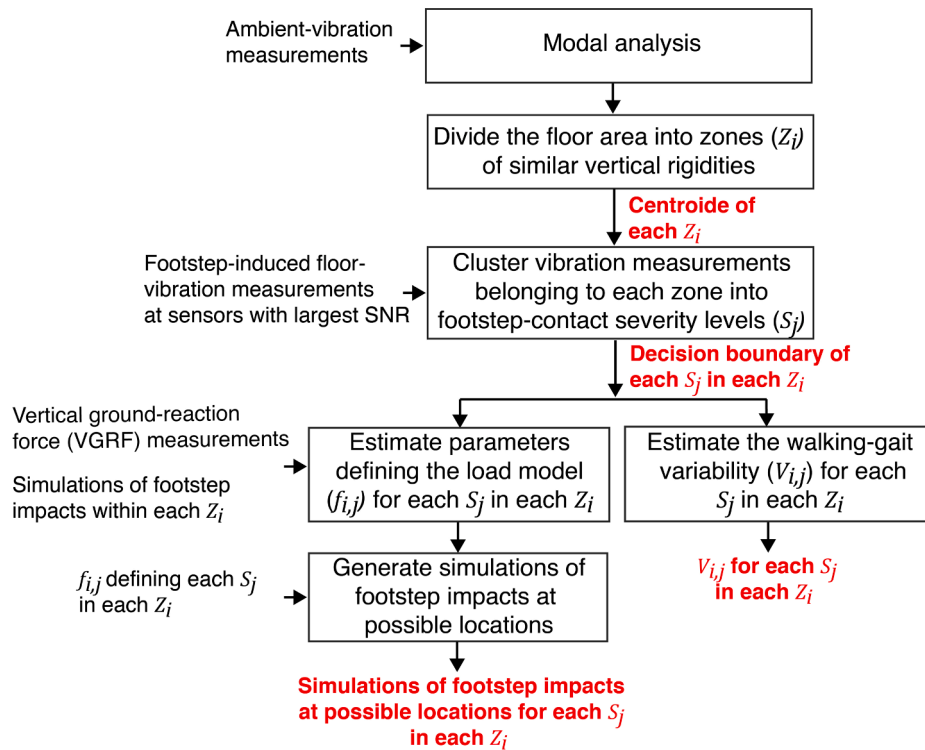
Fig. 4. Strategy for footstep-impact simulations.

clusters (see Section 4.3.2).

Standard deviation (σ) and the maximum difference in amplitude (Δ_{amp}) of footstep-impact signals recorded at the sensor with largest signal-to-noise ratio (SNR) are used as features for clustering. The sensor with largest SNR to a footstep impact is assumed to have a maximum value of σ of the event signal compared with other sensors. Δ_{amp} and σ values are well-suited to clustering since they are correlated to the impact force that is induced by footsteps.

Footstep-impact signals are decomposed, using continuous wavelet transform (CWT), and reconstructed, using inverse wavelet transform (IWT), at a frequency range that contains the first few bending modes of the structure. The Morlet wavelet [66] is used as the mother wavelet due to its shape similarity to the footstep-impact signal. Prominent peaks in the singular values of CPSD from ambient vibration analysis helps delimit the frequency range with most energy contribution. Use of wavelet transforms enhances the SNR of footstep-even signals, which improves clustering results.

Footstep-event signals belonging to each contact-severity (S_j) level in each zone (Z_i) are used to estimate their corresponding walking-gait variability ($V_{i,j}$). Relative $V_{i,j}$ is estimated based on comparing σ of processed event signals (belonging to each S_j level of each Z_i) from the same footstep-impact location with their mean values. Bounds corresponding to the 99th percentile of the distribution of the resulting statistics are used to define a uniform distribution for each $V_{i,j}$.

Clusters defining S_j levels in each Z_i are used to estimate parameter values defining each load model ($f_{i,j}$ in Eq. (5)) based on finite element simulations induced by footstep impacts. The load model involves several parameters (including forces and durations). The value range of each parameter is taken from Table 1.

Simulations of footstep at the same locations used to define contact-severity (S_j) levels within each zone (Z_i) are generated using possible combinations of parameter values that characterize the load model (Eq. (5)). Parameters that contribute the most to the load function (sensitivity greater than 5 %, see Section 4.2) are used to define the load model ($f_{i,j}$). The minimum, maximum and mean values of each parameter are used in simulations as a sampling strategy. Decision boundaries

resulting from clustering vibration measurements of each Z_i are used to separate the footstep-impact simulations into groups defining each S_j level. Average values of each parameter corresponding to footstep-impact simulations that belong to each S_j level in each Z_i define each load model ($f_{i,j}$).

Footstep impacts at possible locations of floor slab are simulated using the predefined load model ($f_{i,j}$) for each contact-severity (S_j) level within each zone (Z_i). Finally, the centroid of each predefined Z_i area, decision boundaries defining each S_j level, estimated walking-gait variabilities ($V_{i,j}$) and footstep-impact simulations using all load models, $f_{i,j}$, are used as inputs for the zone-based occupant localization strategy (see Fig. 5).

3.5. Zone-based occupant localization

Zone-based occupant localization employs prior information of footstep-contact dynamics (see Section 3.4). Model-based occupant localization incorporates physics-based models to infer possible locations of an occupant from detected footstep-event vibrations (see Fig. 1). Relevant steps involved in the zone-based occupant localization strategy are shown in Fig. 5.

The inputs to the methodology in Fig. 5 are footstep-event signals. These signals, captured at each sensor location, are decomposed using CWT and reconstructed using IWT at frequency range that covers the first few bending modes of the floor slab. Standard deviations, σ, of the footstep-event signals, captured at sensor locations, are compared with model simulations for occupant localization.

The floor is decomposed into a grid of possible locations based on the average distance between two footsteps. These potential locations are used to simulate footstep impacts using a finite element model. Simulated footstep-event signals are decomposed and reconstructed at the same frequency range that is used to process the vibration measurements. Standard deviations, σ, of the processed and simulated signals are retrieved for occupant localization.

EDMF, as described in Section 3.1, is applied to identify a population of possible locations of occupants. The model falsification approach
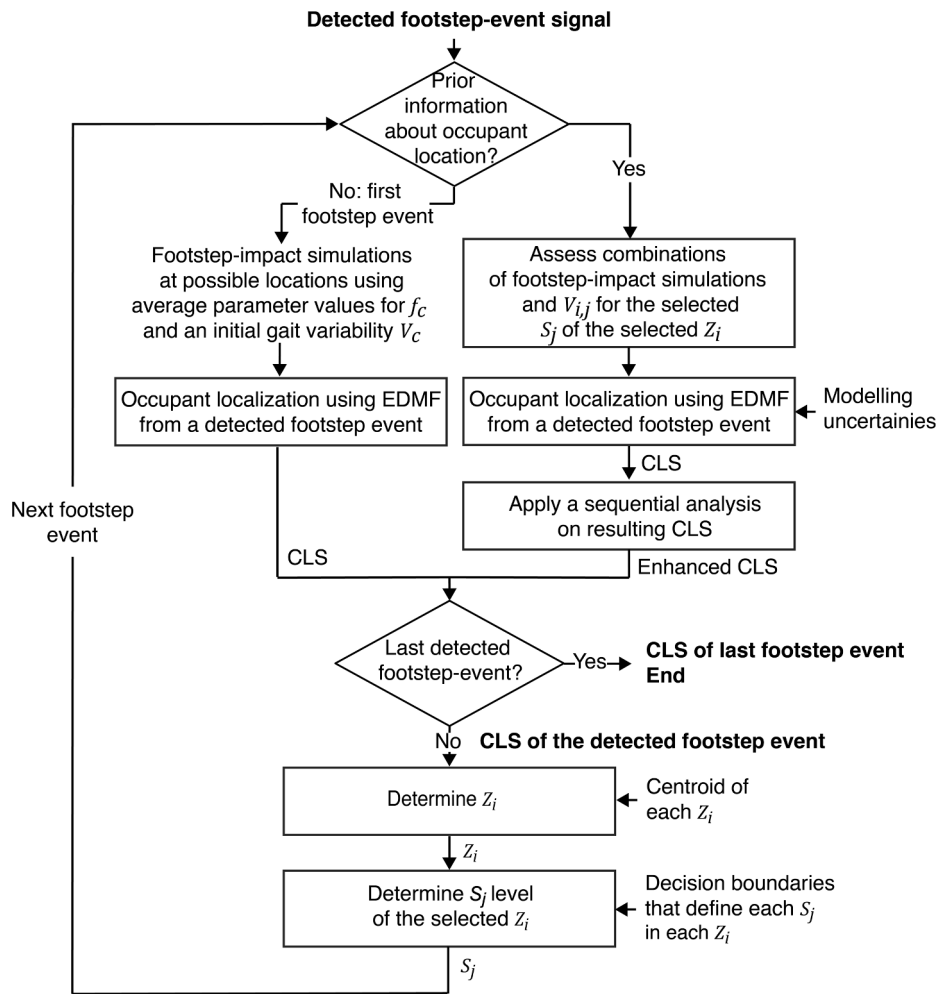
Detected footstep-event signal

Fig. 5. Zone-based occupant localization strategy. CLS is candidate location set.

explicitly incorporates measurement and model uncertainties from various sources. Model uncertainties that include model imperfections and unknown model parameters such as those describing the load model, material properties and stiffness of support conditions are estimated based on engineering judgment [31,57,67] and prior observations. Measurement uncertainties include resolution and precision of sensors and variability in gaits of occupants walking along the same trajectory multiple times. Variability in walking gait, due to the natural variability of occupant anatomies, walking speed and type of shoes, are quantified using prior measurements (see Section 3.4).

For the first detected footstep event, initial simulations are carried out using average values of parameters that define the load model (f_c) for localization using EDMF. These parameters are determined based on prior analysis of VGRF measurements (see Section 4.3.2). An initial walking-gait variability (V_c) is estimated based on prior footstep-impact vibrations from several occupants walking on the same locations with the same speed repeated multiple times (see Section 4.3.2). f_c and V_c are used only for commissioning since prior information of occupant location is not available.

Subsequently, the resulting CLS is used to ascertain the zone (Z_i) that defines the floor response due to the detected footstep event. The zone, Z_i, whose centroid is closest to the centroid of the resulting CLS is selected. Signal of the detected footstep event at the closest sensor location is used to determine the contact-severity (S_j) level (cluster #) using decision boundaries defining clusters within the selected Z_i. The sensor with the largest SNR signal to a footstep impact is assumed to have a maximum σ of the event signal compared to other sensors. De-

cision boundaries defining each S_j level within each Z_i are predetermined for zone-based occupant localization (see Section 3.4).

Knowledge of the contact-severity (S_j) level within the selected zone (Z_i) helps select an appropriate load model ($f_{i,j}$) for simulations and appropriate walking-gait variability ($V_{i,j}$) (for example, see Tables 4 and 5). The footstep-impact simulations that correspond to the selected $f_{i,j}$ and $V_{i,j}$ are used for localizing the succeeding footstep event using EDMF.

Selected $V_{i,j}$ are combined with predefined modeling uncertainties to estimate the localization thresholds. These thresholds are used to select the location instances whose footstep-impact simulations that are generated using the selected $f_{i,j}$ that do not contradict the measured footstep-event signal. Once information of possible locations from a preceding footstep event is available, the CLS of the current footstep event is enhanced using a sequential analysis [31,32].

The sequential analysis combines information about consecutive footsteps to reduce ambiguity within the CLS of footstep events. Based on information about the previous footstep event, it is assumed that the distance of two consecutive footstep impacts cannot exceed a predefined distance such as the average length of a step (approximately 75 cm). Thus, when the minimum distance between a candidate location (resulting from EDMF) of a current footstep event and CLS of the preceding footstep event is greater than a predefined distance, the candidate location is rejected. This localizing strategy is carried out interactively for each footstep event.
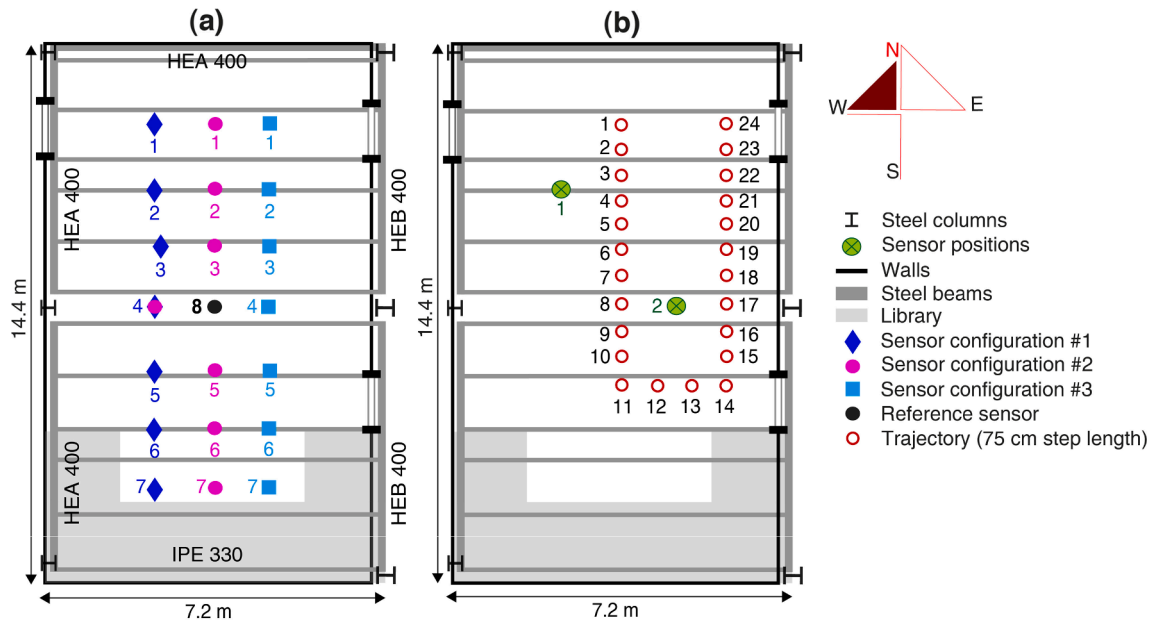
Fig. 6. Occupant localization using a zone-based approach is tested on a full-scale concrete slab. (a) In an initial commissioning stage, three sensor configurations (eight sensors each) are used to record ambient vibrations of the floor slab for modal analysis. Diamond, circle, and square markers represent sensor configurations #1 to #3. Sensor 8 is used as a reference to assess the mode shapes of the floor slab using the three sensor configurations. (b) In the in-service phase, two sensors capture vibration measurements from five occupants walking individually along a fixed trajectory multiple times (one occupant at a time).

4. Full-scale case-study

Strategies described in Section 3 for assessment of footstep-contact dynamics and zone-based approach for increasing localization precision of occupants are illustrated and evaluated in the following sections using a full-scale case study. The full-scale case study is a floor slab (approximately 100 m²) of a building located in Switzerland. The floor is a reinforced concrete slab that is is 20 cm thick with linoleum finishing. Apart from the high stiffness of the slab, a dense network of steel beams underneath the slab results in relatively short spans, as shown in Fig. 6.

The steel frame is composed of five H-beams on the north, west-and-east ends, and 12 I-beams. The floor is supported by six steel columns. A non-structural wall made of plasterboard is above the structure on the east end. The lower half of the west end and the south end of the slab are connected to prefabricated reinforced concrete structural walls. Remaining parts of the slab are joined to structural masonry walls.

Several uni-directional vibration sensors (Geophones SM-24 by I/O Sensor Nederland) are used to measure vertical velocity-response of the slab. An acquisition unit (NI USB-6003) is used to capture the vibration measurements with a sampling rate of 1000 Hz. In Fig. 6a, eight vibration sensors following three configurations are used for modal analysis of the floor slab. Sensors are placed in the initial commissioning phase to cover the entire floor space. The sensor is placed at mid-span of the floor (see Sensor 8 in Fig. 6a) is used as a reference to quantify the vertical mode shapes. Ambient vibrations are recorded for 20 min for each set of sensors.

Only two vibration sensors are placed on the floor slab to capture vibration response from occupants walking in the instrumented space for the in-service phase, as shown in Fig. 6b. One sensor is placed at

quarter-span and another at mid-span of the floor to cover the two-thirds of the floor-area (approximately 70 m²) for footstep-contact-dynamics determination. Accounting for the library at the south end of the slab (see Fig. 6), this area covers most of the available space for occupant movement. These sensors are placed based on the dominant vertical bending modes of the floor slab (one sensor per ∼ 35 m²).

Use of a sparse sensor configuration for occupant localization on a rigid floor slab is complex and little research is available regarding such cases. Prior empirical analysis on a similar floor slab belonging to the same building has been used to demonstrated the need for physics-based models for localization [36]. Therefore, this case study demonstrates a bound for useful application of the model-based occupant localization methodology.

Based on prior observations, step length is found to vary between approximately 60 cm and 90 cm with respect to the walking-speed level (from slow to fast walking) [43]. In this paper, an average step length of 75 cm is chosen for walking tests.

Vibration measurements are recorded from five occupants walking individually along a fixed trajectory (see Fig. 6b) multiple times. Information related to occupant weights and heights are presented in Table 2. Occupants have walked along fixed footstep-impact locations (24 locations separated by 75 cm as step length) and at fixed speeds. The test for each occupant walking is repeated with two types of shoes (hard-and-soft soled shoes) and five speeds. Walking speeds (in terms of steps per second) are 1.4 Hz; 1.6 Hz; 1.8 Hz; 2 Hz and 2.2 Hz. Measurements are repeated on average 14 times for each occupant wearing a particular shoe type and walking at the same speed. For each impact location, an average of 700 measurements are recorded. These measurements are used to determine footstep-contact dynamics and estimate the variability in walking gaits.

Additional vibration measurements recorded from the same sensor layout presented in Fig. 6b are used to test the zone-based occupant localization approach. These measurements are from the same occupants (see Table 2) walking individually along the same trajectory (see Fig. 6b). Each occupant walks at the same speed levels (1.4 Hz; 1.6 Hz; 1.8 Hz; 2 Hz and 2.2 Hz) leading to 25 walking tests.

Table 2
Occupant weights and heights.

Occupant	Weight (Kg)	Height (cm)
O1	92	178
O2	70	180
O3	87	181
O4	67	164
O5	58	173

4.1. Numerical simulation using a finite-element model

Footstep-impacts are simulated using a finite-element model of the floor slab (see Fig. 6b) subjected to a load model as described in Eq. (5). Linear modal superposition is used to calculate the dynamic response caused by footstep impacts using ANSYS [68]. The floor slab is modeled using shell elements (SHELL181) and beams are modeled as beam elements (BEAM188). Beam elements are assumed to be fully connected to the shell elements. Also, columns are modeled as simple supports (see Fig. 6). The elastic moduli for the steel and the concrete slab are taken to be 210 and 35 GPa.

Due to incomplete knowledge of boundary conditions of the floor slab, the separation walls (see Fig. 6) are modeled using translational zero-length springs in the vertical direction (COMBIN14). Four spring elements are involved in the finite element model to describe the upper half of the west end of the slab (masonry wall), the lower half of the west end and the south end of the slab (reinforced concrete walls), the east end of the slab (plasterboard walls), and the north end the slab (masonry wall that is connected to a concrete staircase), as illustrated in Fig. 6b.

Stiffness values of these springs are estimated based on prior sensitivity analysis. Latin-hypercube sampling approach [69] is used to generate 500 spring-stiffness values from sufficiently small to sufficiently large. Values of each spring element are varied at a time using modal analysis simulations. This analysis results in an s-shaped function of the fundamental frequency as a function of each spring stiffness. The stiffness values between freely supported and completely fixed of all spring elements are 316 N/mm, 631 N/mm, 1259 N/mm and 200 N/mm respectively.

The room furniture and the linoleum floor finishing are not taken to account in the finite element model of the floor slab. Based on prior modal analysis using ambient vibration measurements (see Section 4.3.1), these elements do not affect the dynamic response of the model in this case.

4.2. Sensitivity analysis of floor vibrations to load function parameters

A sensitivity analysis of normalized load model (Eq. (5)) parameters (see Table 1) to vary between -1 and 1 is conducted to evaluate the influence of each parameter on the simulated floor responses. Sensitivity analysis is carried out using linear regression [70] with Δ_{amp} and σ as response and parameters of the load model as regressors. Footstep-impact simulations using the load model (Eq. (5)), are carried out for one footstep location (footstep #4 in Fig. 6b) using a finite element model of the floor slab, as described in Section 4.1. Latin-hypercube sampling approach [69] is used to generate 1000 combinations of the parameters of load model.

Sensitivity of floor-vibration response to load-model parameters that include bodyweight, forces F1 to F5 and durations T1 to T3 (see Table 1)
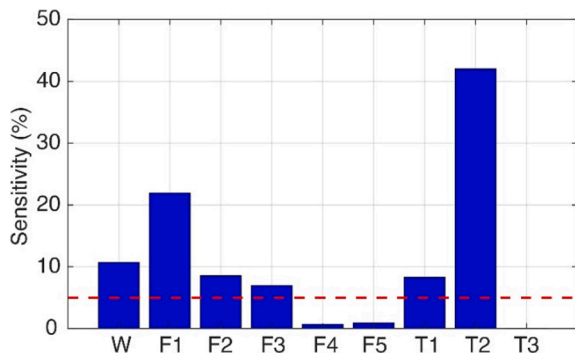

Fig. 7. Sensitivity analysis of normalized load model (Eq. (5)) parameters (see Table 1) to Δ_{amp} and σ of the simulated footstep-impact signals at one footstep location.

are shown in Fig. 7. Several sources, including occupant weight, height, and walking speed, contribute significantly to the variability in walking-gait patterns. These walking-gait variabilities are reflected in the distribution of parameter values of the load model, as shown in Table 1.

Distribution bounds that are presented in Table 1 are used to generate load models for footstep-impact simulations. Based on sensitivity analysis, as shown in Fig. 7, forces F1, F2 and F3, durations T1, and T2, as well as W (Eq. (5)) are found to significantly influence the simulated footstep-impact signals (sensitivity greater than 5 %) compared with forces F4 and F5, and Duration T3 (Eq. (5)).

Among the most significant parameters, initial heel-contact force (F1) and duration of the full heel-contact (T2) affect the most the simulated footstep-impact responses. Therefore, the heel phase of walking gait (see Fig. 3) dominates the response of simulated footstep-impacts compared with the heel-to-toe phase and the toe-off phase. Sensitivities of forces F4 and F5, as well as Duration T3 on the simulated footstep-impact signals are less than 5 %. Thus, F4, F5 and T3 are fixed to their mean values for subsequent footstep-impact simulations for model-based localization (see Section 3.5).

4.3. Determination of footstep-contact dynamics on a full-scale floor slab

4.3.1. Defining zones of similar vertical rigidity

Determination of footstep-contact dynamics starts with a modal analysis to define zones with similar rigidities, as shown in Fig. 4. Ambient vibrations recorded by three sensor configurations (see Fig. 6a) are processed using CPSD, as described in detail in Section 3.4. The first singular decomposition of the resulting CPSD for each sensor configuration reveals the modes with most energy contribution to vertical bending. These modes are contained within the frequency range of 10–40 Hz. The first and the second vertical bending modes are at frequencies 15.5 Hz and 24 Hz.

FDD resulting from ambient vibrations recorded from each sensor configuration is carried out to determine the mode shapes that correspond to the first and second vertical bending modes (see Section 3.4). The amplitude of the deformed-shape at each sensor location is normalized by the deformed-shape amplitude given by the reference sensor (see Sensor 8 in Fig. 6a). Fig. 8 presents deformed-shape patterns of the first and second fundamental modes of the floor slab. In Fig. 8, boxes represent the steel columns. Dashed lines represent the continuity of the slab. Diamonds, circles, and squares represent amplitudes at positions defined by sensor configurations #1 to #3 (see Fig. 6a). zones Z_1 to Z_3 illustrate the floor areas that present similar structural rigidities.

The mode-shape of the floor slab governed by the first vertical mode at 15.5 Hz is shown in Fig. 8a. The maximum deformation of the first mode-shape is located at quarter-span of the floor slab. The south part of the slab (see Fig. 8) has less deformation compared with the north part due to the connection of the slab to reinforced concrete walls. The mode-shape of the floor slab governed by the second vertical mode at 24 Hz is shown in Fig. 8b. The maximum deflection of the second mode-shape is located at mid-span of the floor slab.

The number of zones with similar rigidities is determined based on the first and the second bending modes of the floor slab (see Section 3.4). For this case study, the floor is divided into three zones of similar structural rigidities, Z_1, Z_2 and Z_3. Zones Z_1 and Z_2 in Fig. 8a define the quarter-and-three-quarters of the floor slab that are primarily affected by the first vertical mode of the structure. Zone Z_2 in Fig. 8b is the floor area (mid-span of the floor) that is governed by the second vertical mode. Zones Z_1 to Z_3 thus describe the spatial characteristics of the structural contribution to footstep-contact dynamics (see Fig. 4).

4.3.2. Determining footstep-contact dynamics

Vibration measurements induced by footstep impacts at locations within each zone (Z_i) (see Fig. 8) are used to define three contact-severity (S_j) levels (low, medium and hard) using k-means clustering, as described in Section 3.4. Values for Δ_{amp} and σ of decomposed (using
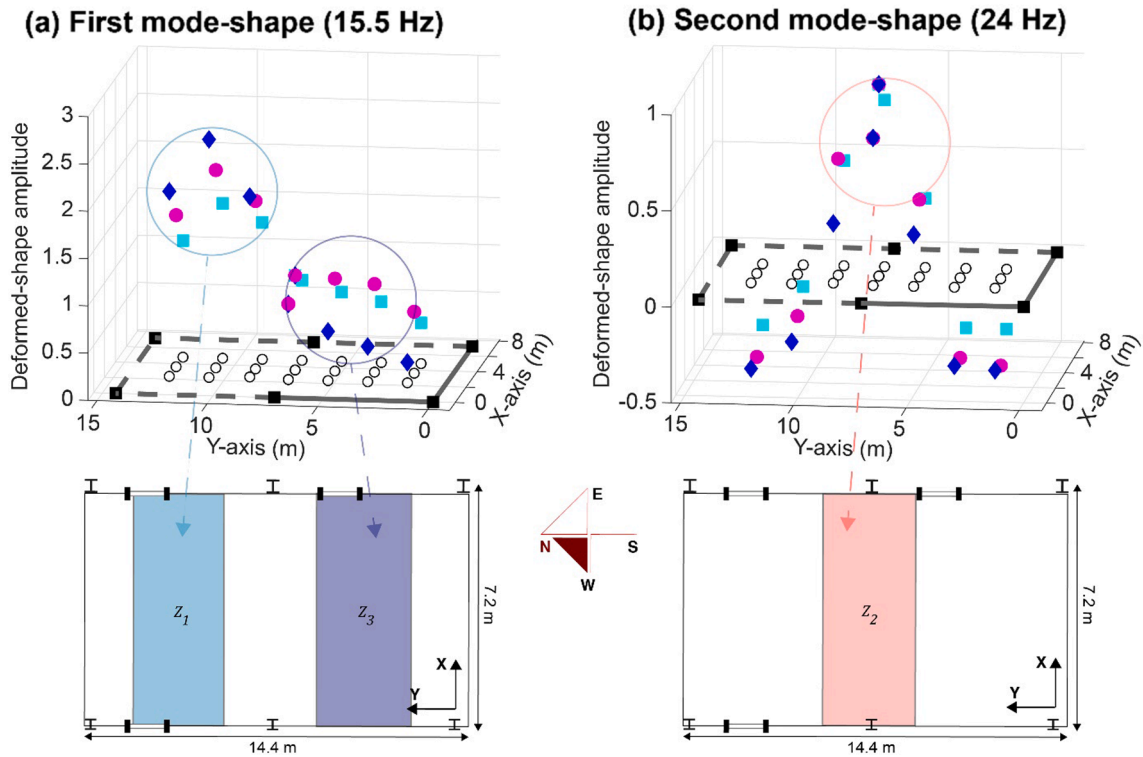
Fig. 8. Deformed-shape amplitudes that are assessed using the FDD approach that correspond to probable modes at frequencies of 15.5 Hz (a) and 24 Hz (b).
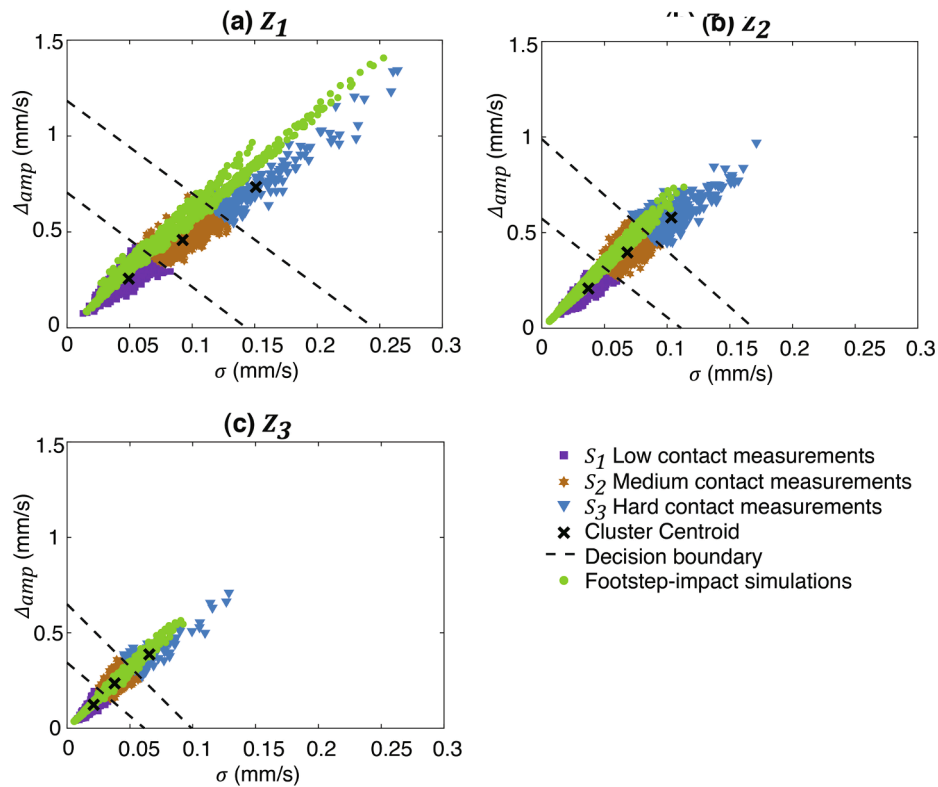

Fig. 9. Clustering vibration measurements into three contact-severity ($S_{j=1..3}$) levels (low, medium and hard) for each zone (Z_i) using *k*-means. Footstep-impact simulations (represented by dots) are carried out using the load model for multiple combinations of parameter values (see Eq. (5) and Table 1).

CWT) and reconstructed (using IWT) footstep-impact signals at a frequency range of 10–40 Hz are used for clustering (see Fig. 4). Footstep-event signals recorded at the sensor with the largest SNR response are

taken into account for clustering (see Fig. 4).

Footstep-induced floor vibrations at locations #3 and #4 (Fig. 6b) are used to define S_j levels for Zone Z_1. Floor vibrations induced by

footstep impacts at locations #8 and #9 (see Fig. 6b) are used to define S_j levels for Zone Z_2. Floor vibrations induced by footstep impacts at locations #12 and #13 (see Fig. 6b) are used to define S_j levels for Zone Z_3. Two consecutive footstep locations inside each zone, Z_i, indicate the inherent variability in walking gait from the right and the left foot of each individual. Taking into account vibration measurements from footstep impacts at two locations for each zone, Z_i, an average of 1400 footstep-event signals from multiple occupants walking at varying speeds with different shoe types are provided as inputs for clustering (see Fig. 4).

Clustering results of the processed footstep-event signals that belong to each zone, Z_i, are shown in Fig. 9. Dashed lines, in Fig. 9, define the decision boundaries that separate contact-severity (S_j) levels in each Z_i. Data points represented by squares are within a region of low contact severity S_1. Data points represented by stars are within the region of medium contact severity S_2. Data points represented by triangles are within the region of hard contact severity S_3. Clustering results show that the regions of data points that define all $S_{j=1..3}$ levels for each Z_i are not the same. This is due to the influence of structural behavior on vibration measurements (location information).

Parameters of the load model (Eq. (5)), that have sensitivities of more than 5 % (see Section 4.2) are taken as potential variables (forces F1 to F3 and durations T1 and T2 in Table 1). Footstep-impact simulations belonging to each zone (Z_i) are generated at locations that are used for clustering the measured vibrations. The minimum, maximum and mean values of each parameter of the footstep-impact load function are used in simulations as a sampling strategy (see Section 3.4). Simulated footstep-event signals belonging to each zone, Z_i, are processed similarly using CWT to extract single components at frequency range of 10–40 Hz. Δ_{amp} and σ values of the processed simulated signals are represented with dots in Fig. 9.

Significant variability, in Fig. 9, is observed for vibration measurements induced by footstep impacts at the same locations (belonging to each zone, Z_i). The uncertainties are from inherent variability in walking gaits between individuals (see Table 1). Also, several factors such as walking speeds and type of shoes add to the variability in walking gait. Significant variability is also observed in the response of footstep-impact simulations at the same locations, belonging to each zone, Z_i, for varying footstep load parameters. Footstep-impact simulations (represented by dots in Fig. 9) carried out using the footstep-impact load function for multiple combinations of parameter values show similar scatter as observed from vibration measurements recorded within each zone, Z_i.

Decision boundaries defining contact-severity (S_j) levels in each zone (Z_i) are used to quantify the dynamics of footstep-contact, including the effect of variability in the load model ($f_{i,j}$) and walking-gait ($V_{i,j}$), as shown in Fig. 4. Also, the resulting decision boundaries help determine the severity level that a footstep event belongs to for the zone-based occupant localization operation (see Section 3.5). Decision boundaries, as functions of Δ_{amp} and σ, are presented in Table 3.

Processed footstep-event signals belonging to each contact-severity (S_j) level in each zone (Z_i) are used to estimate the walking-gait vari-

Table 3
Decision boundaries defining each contact-severity (S_j) level in each zone (Z_i).

Zone	Severity level	Decision boundary
Z_1	S_1	$\Delta_{amp} \leq -4.9\sigma + 0.7$
	S_2	$\Delta_{amp} > -4.9\sigma + 0.7\Delta_{amp} \leq -4.8\sigma + 1.2$
	S_3	$\Delta_{amp} > -4.8\sigma + 1.2$
Z_2	S_1	$\Delta_{amp} \leq -5.1\sigma + 0.6$
	S_2	$\Delta_{amp} > -5.1\sigma + 0.6\Delta_{amp} \leq -5.9\sigma + 1.0$
	S_3	$\Delta_{amp} > -5.9\sigma + 1.0$
Z_3	S_1	$\Delta_{amp} \leq -5.6\sigma + 0.3$
	S_2	$\Delta_{amp} > -5.6\sigma + 0.3\Delta_{amp} \leq -6.5\sigma + 0.7$
	S_3	$\Delta_{amp} > -6.5\sigma + 0.7$

Table 4
Relative walking-gait variability ($V_{i,j}$) for each contact-severity (S_j) level in each zone (Z_i). Walking gait variability is quantified as a uniform probability distribution with minimum and maximum bounds of the distributions for various scenarios shown in the table.

		Min (%)	Max (%)
Z_1	$V_{1,1}$	−53.1	55.8
	$V_{1,2}$	−37.5	33.5
	$V_{1,3}$	−62.3	24.9
	V_1(without clustering)	**−138.9**	**71.0**
Z_2	$V_{2,1}$	−51.3	58.8
	$V_{2,2}$	−49.3	28.1
	$V_{2,3}$	−31.6	29.7
	V_2(without clustering)	**−129.5**	**74.1**
Z_3	$V_{3,1}$	−55.4	52.2
	$V_{3,2}$	−83.9	32.2
	$V_{3,3}$	−46.2	30.4
	V_3(without clustering)	**−190.4**	**72.8**
V_c(without zoning)		**−71.9**	**53.6**

ability ($V_{i,j}$) , as shown in Fig. 4. For data points belonging to a particular S_j level within a particular Z_i, the relative $V_{i,j}$ is estimated based on comparing the σ of processed event signals from repeated footstep impacts at fixed impact location with the mean σ value. Since measurements from two footstep-impact locations are used for clustering, statistics resulting from data points from both locations are combined.

Bounds defining 99th percentiles of the resulting distribution are used to define a uniform distribution for each variability, $V_{i,j}$, as shown in Table 4. A conservative uniform distribution is assumed due to the lack of more precise information about true probability distributions. Similarly, the processed footstep-event signals belonging to each zone, Z_i, are used to determine the bounds of a uniform distribution for the variability in walking gait (V_i), without considering clustering results (see Table 4).

Defining groups of contact-severity (S_j) levels in each zone (Z_i) leads to a significant reduction in variability from walking-gait patterns (multiple individuals, shoe types, etc.), as shown in Table 4. The relative bounds of the resulting distribution for each walking-gait variability ($V_{i,j}$) assessed for each S_j level in each Z_i present a significant reduction (from 45 % to 70 %) compared with walking-gait variabilities ($V_{i=1..3}$) that are assessed using only zoning.

According to the zone-based occupant-localization strategy (see Fig. 5), when prior information of occupant location is not available (first detected footstep event), an initial walking-gait variability (V_c) is used to define the localization thresholds (Eqs. (3) and (4) in Section 3.1). Variability, V_c, is estimated based on comparing the σ of processed event signals from the same footstep-impact location induced by an occupant wearing a particular type of shoe and walking at a particular speed with the mean σ value. Statistics are computed individually for each occupant at several footstep-impact locations (locations #2, #4, #6, #8, #10, #12, #13, #15, #17, #19, #21 and #23 shown in Fig. 6b) without zoning.

Combining statistics from each occupant walking at each speed at each impact location, the bounds of the initial walking-gait variability, V_c, vary between −72% and 54%, as shown in Table 4. The initial walking-gait variability, V_c, is a conservative estimate that assumes only the inherent variability in walking gait without accounting for external factors such as walking speeds and type of shoes. Thus, the walking-gait variability, V_c, is used only for localizing the first detected footstep (see Fig. 5).

Decision boundaries resulting from clustering of vibration measurements for each zone (Z_i) are used to separate the footstep-impact simulations into groups defining each contact-severity (S_j) level. Parameters defining each load model ($f_{i,j}$) are subsequently determined

Table 5
Footstep load function ($f_{i,j}$) parameters for each contact-severity (S_j) level in each zone (Z_i).

	$f_{1,1}$	$f_{1,2}$	$f_{1,3}$	$f_{2,1}$	$f_{2,2}$	$f_{2,3}$	$f_{3,1}$	$f_{3,2}$	$f_{3,3}$	f_c
W (kg)	72.4	75	80	73.2	76.2	86	73	74.2	82	75
F1 (kg)	24	36	33.4	28	34.3	32.2	25.2	35.6	33	30
F2 (kg)	18.2	27.1	24.3	21.2	25.5	22.6	19.1	26.9	23.8	22.5
F3 (kg)	89.3	92	105	90.3	94.7	122	90.6	98.3	109.6	93.7
T1 (s)	0.027	0.021	0.027	0.027	0.021	0.025	0.028	0.02	0.025	0.025
T2 (s)	0.15	0.12	0.07	0.15	0.07	0.04	0.16	0.09	0.05	0.12

using the clustered footstep-impact simulations (see Fig. 4). Average values of the possible sets of each parameter corresponding to footstep-impact simulations of each S_j level in each Z_i define each load model, $f_{i,j}$. The resulting parameters that define each load model, $f_{i,j}$, are presented in Table 5. Footstep impacts at possible locations of floor slab are then simulated using the defined load model, $f_{i,j}$ (see Section 4.1). These simulations are used to perform the zone-based occupant localization (see Section 3.5).

Referring to the zone-based occupant localization strategy, explained in Section 3.5, localization of the first detected footstep event involves the simulation of footstep impacts using an initial load model (f_c). Parameter values that define the load model, f_c, are the average values of the extended parameter distribution, as shown in Table 1. Average values of parameters that define the initial load model, f_c, are presented in Table 5.

4.4. Zone-based occupant localization application on full-scale floor slab

The zone-based approach incorporates prior information of footstep-contact dynamics (based on zoning according to structural behavior) to improve precision of occupant localization, as described in Section 3.5. Localization of a walking occupant is performed independently for each captured footstep-event signal (see Fig. 5). Candidate-location set (CLS) for each detected footstep event is obtained using EDMF by combining information from each sensor location (Eq. (4) in Section 3.1). Standard deviation values (σ) of measured and simulated footstep-event signals at sensor locations are used as metrics for the falsification process. In Eq. (4), measured signal standard deviation is $m_{l,e}$ and simulated footstep standard deviations are $g_l(\theta)$ where l is sensor location and e is detected event. Using the falsification process, model instances that contradict footstep-induced floor vibration measurements are rejected.

A sequential analysis that accommodates information about previous footsteps is used to enhance the precision of the CLS of a current footstep event (see Section 3.5). The centroid of the resulting CLS of a current footstep event from EDMF is used to determine the zone (Z_i) of the detected footstep impact (see Fig. 5). Then, Δ_{amp} and σ of decomposed (using CWT) and reconstructed (using IWT) footstep-impact signals are used to define the contact-severity (S_j) level based on decision boundaries defined in Table 3. Corresponding to the level of contact severity, S_j, appropriate simulation model ($f_{i,j}$) and walking-gait variability ($V_{i,j}$) are used for EDMF to generate CLS for the next captured footstep event.

Vibration measurements from five occupants (see Table 2) walking individually along a fixed trajectory (see Fig. 6b) are used to test the improvement of the model-based occupant localization using the zone-based approach (see Fig. 5). Each occupant walks at five speed levels (1.4 Hz; 1.6 Hz; 1.8 Hz; 2 Hz and 2.2 Hz). The type of shoes during these walking tests is not fixed.

4.5. Model predictions

The first step in model-based occupant localization involves generating footstep-impact simulations using a finite element model of the floor slab (see Fig. 6b), as described in Section 4.1. Two-thirds of the floor slab is divided into a grid of possible locations. Regarding the assumed step length of 75 cm for measurements (see Section 4), the

distance between two possible locations for model simulations is assumed to be 37.5 cm (half of the assumed step length). This leads to 432 possible footstep locations. This provides a fine grid sampling for exhaustive search of candidate locations using model falsification (Eq. (4) in Section 3.1). Regarding each possible location, simulated signals are extracted at sensors 1 and 2, as shown in Fig. 6b.

In the zone-based occupant localization strategy (see Fig. 5), when prior information about occupant location (first captured footstep event) is not available, simulations are carried out using average values of parameters that define the initial load model, f_c (see Table 5). Simulations at predefined locations are repeated for each load model ($f_{i,j}$) defining each contact-severity (S_j) level for each zone (Z_i). Predefined footstep-contact dynamics based on zoning according to structural behavior and clustering footstep-induced floor vibrations are involved in determining load models, $f_{i,j}$ (see Table 5).
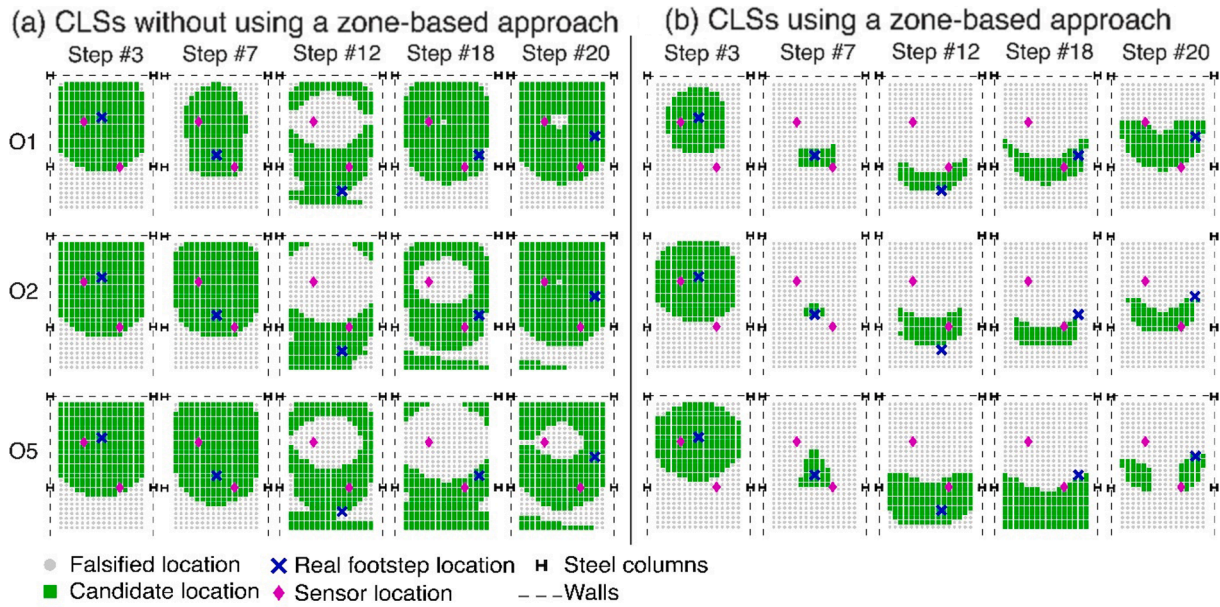
4.6. Uncertainty estimation

Model simulations are prone to uncertainties from sources such as model imperfections (idealized boundary conditions and omissions), unknown model parameters and idealized load model (Eq. (1) and (2) in Section 3.1). The finite element model of the floor-slab (see Fig. 6) involves several simplifications including the use of shell elements for the concrete slab and one-dimensional bar elements for the supporting beams. Also, model simplification includes the use of translational springs (rotation free) to model the plasterboard, masonry and reinforced concrete walls (see Fig. 6). The finite element model does not include elements such as the room furniture, linoleum floor finishing and connections (in the horizontal direction) between the floor slab and the reinforced concrete walls (see Section 4.1).

In addition, the footstep-impact load function (Eq. (5)) is applied independently to a single node in simulations at each predefined location. This excludes contribution of the other foot during the pre-swing phase of the gait pattern (see Fig. 3) (the two feet are in contact with the ground). This further increases the uncertainty associated with the simulation model. Based on engineering judgment and heuristics [31,67,71], uncertainties related to model simplifications and omissions are biased and estimated to be uniformly distributed between −15% to +25% of simulated amplitudes.

According to sensitivity analysis of the applied load model, the heel phase is the most important stage, as presented in Section 4.2. The frequency of the heel phase (1/duration) of the applied load function operates with low-frequency components (see Table 5). Since these frequency ranges fall within the range of natural frequencies of the structure, low-frequency components of simulated footstep-event signals are affected [31]. This results in over-estimated (biased) simulated velocity amplitudes, thereby leading to additional model uncertainties of −30 % to 0 %.

Measurements are affected by uncertainties from sensor resolution, precision and variations in floor vibrations due to natural variability in walking gaits (Eqs. (1) and (2) in Section 3.1). Sensor resolution and precision provided by the sensor manufacturer are not significant (approximately 2 %). According to the zone-based occupant localization strategy (see Fig. 5), when prior information about occupant location (first captured footstep event) is not available, an initial walking-gait

Fig. 10. Candidate-location sets (CLSs) that correspond to footstep locations #3, #7, #12, #18 and #20 (see Fig. 6b) result in localization of footstep events of occupants O1, O2 and O5 (see Table 2). Localization precision refers to the percentage of falsified locations from all possible locations (432 possible locations). CLSs that are obtained using a zone-based occupant localization approach (b) are more precise than those obtained using only EDMF and a sequential analysis (a) (see Section 4).

variability, V_c, is used for localization (see Table 4). Inherent variability in walking gait ($V_{i,j}$), resulting from several individuals walking at various speeds and wearing various type of shoes are determined prior to zone-based occupant localization. Walking-gait variability ($V_{i,j}$) defining each contact-severity (S_j) level in each zone (Z_i) are quantified as shown in Table 4.

Subsequently, model and measurement uncertainties related to each detected footstep event are combined using Monte-Carlo sampling with one million samples, as explained in Section 3.1. Based on a target reliability of localization of 95%, localization thresholds for each detected footstep event are derived from the combined uncertainty ($U_{c,l}$ in Eq. (3)).

4.7. Zone-based occupant localization results

In Fig. 10, CLSs of few footstep events for occupants, O1, O2 and O5 (see Table 2) walking along a trajectory (see Fig. 6b) are shown. For the results shown in Fig. 10, occupants O1, O2 and O5 are walking at a frequency of 1.8 Hz. During these walks, occupants O1 and O2 wear hard-soled shoes while occupant O5 wear soft-soled shoes. Measurements for localization of these occupants are recorded using two vibration sensors (see Fig. 6b).

Footstep-impact events at locations #3 and #20 lie within Zone Z_1, locations #7 and #18 lie within Zone Z_2, and Location #12 lies within Zone Z_3 (see Fig. 6b). CLSs that result from the zone-based occupant localization operation are illustrated in Fig. 10b. This approach incorporates predefined footstep-contact dynamics for occupant localization using EDMF and a sequential analysis.

Resulting CLSs are compared with those resulting from only EDMF and sequential analysis (see Fig. 10a). For this operation, footstep-impact simulations are conducted using the load model, f_c (see Table 5) for detected footstep events. The combined uncertainty incorporates the initial walking-gait variability, V_c as defined in Table 4.

In Fig. 10, squares represent the CLSs and dots represent the falsified location sets. Dashed lines represent the walls delimiting the floor slab. Diamonds represent sensor locations and h-shapes represent the steel columns. Also, in Fig. 10, real locations of each footstep event are represented with crosses.

Localization precision refers to the percentage of falsified locations from all possible locations (432 possible locations). For example, precisions of CLSs that correspond to footstep events at locations #3, #7 and # 20 for occupants O1, O2 and O5 are less than 40 % (see Fig. 10a). Also, precisions of CLSs of footstep events #12 and #18, do not exceed 50 %.

Incorporating physics-based models in the interpretation of footstep-event signals using EDMF provides accurate localization results for all footstep events, as shown in Fig. 10. From the results in Fig. 10a, occupant localization has low precision since EDMF incorporates high values of systematic uncertainty and model bias, (see Fig. 10a) to sacrifice precision for accuracy.

Accuracy is determined through comparing the true footstep locations with the resulting CLSs with a tolerance of plus or minus one footstep location. This tolerance is taken since the impact locations during measurements do not coincide necessarily with the initial location set, especially when participants change walking directions at locations #11 and #14 (see Fig. 6b). Thus, for each footstep event, localization is accurate when at least one candidate location is within 0.75 m radius (equal to the distance between two footsteps) from the correct location.

Incorporating the predefined footstep-contact dynamics in model-based occupant localization approach enhances localization results as shown in Fig. 10b. Defining appropriate load models, $f_{i,j}$, for simulations

Table 6

Comparison of accuracy and precision of occupant localization, with and without knowledge of footstep-contact dynamics, for five occupants (O1 to O5 in Table 2).

		O1	O2	O3	O4	O5	Average
Zone-based approach (Section 3.5)	Accuracy (%)	94.2	93.3	94.2	91.7	95	**93.7**
	Precision (%)	71.7	69.5	67.2	70.7	70.9	**70**
No zone-based approach (Section 3.1)	Accuracy (%)	100	100	97.5	99.2	95.8	**98.5**
	Precision (%)	42.5	42.2	50.7	50.2	46.7	**46.5**

(see Table 5) and appropriate walking-gait variabilities, $V_{i,j}$ (see Table 4), leads to an increase in precision of CLSs without compromising accuracy. For example, CLSs of footstep event #7 for occupants O1, O2 and O5 present an increase in precision of more than 100 % compared with using only EDMF and a sequential analysis. Therefore, dividing the floor into zones of similar structural rigidities and clustering the vibration measurements of footstep events belonging to each zone into several contact-severity levels supports the interpretation of measurements.

The average accuracy and precision of localization results (with and without zoning) for each occupant are presented in Table 6. For each occupant, the average accuracy and precision are determined based on CLSs resulting from 24 captured footstep events (see Fig. 6b) repeated at five speed levels (1.4 Hz; 1.6 Hz; 1.8 Hz; 2 Hz and 2.2 Hz).

The average localization accuracy of all occupants, resulting from the zone-based occupant localization approach (~94 %) is marginally less that the one obtained without zoning (~98.5 %), as presented in Table 6. Average localization accuracy per occupant reduces between 1 % and 8 % when using a zone-based occupant localization approach.

The zone-based occupant localization strategy improves localization precision by an average of 53 % compared with localization without zone-based information. The average increase in localization precision per occupant varies between 33 % and 82 %. Defining groups of footstep-contact severity levels in various zones, determined based on the understanding of structural behavior, improves precision of localization using a model-based approach without significantly comprising accuracy.

5. Discussion and future work

Measurements of VGRF induced by footstep impacts (from 12 participants) are used to design a load model based on sine and cosine functions and determine value ranges of load parameters. Several sources, including occupant weight, height, and walking speed, contribute significantly to variability in walking-gait patterns. A sensitivity analysis highlights the most significant parameters for the load model using simulated responses. Using a finite element model, simulations have been generated at sensor locations for footstep-impacts at the same location for varying footstep load models. Moreover, through the sensitivity analysis, the heel phase of the walking gait pattern is confirmed to be the most important stage for the floor response induced by footstep impacts.

Significant variability is observed in measured and simulated responses (at the same sensor location) induced by footstep impacts at the same location. The uncertainties are from inherent variability in the walking style of an individual and variability in gait between multiple individuals. Dividing the floor into zones of similar structural rigidities and clustering vibration measurements of footstep events belonging to each zone into several contact-severity levels helps better assess information regarding variability in walking gait.

Incorporating structural behavior and various sources of uncertainties in occupant localization application using EDMF, footstep events from five occupants have been localized accurately. Based on a two-sensor configuration, a model-based approach (EDMF) that includes zoning according to structural behavior, systematic errors and model bias in the interpretation of vibration measurements leads to more precise results compared with those obtained without zoning. Improvement in localization precision helps identify walking trajectories (Fig. 1).

The numbers of the resulting CLs remain high for several footstep events limiting the precision of occupant locations. As shown in Fig. 10b, footstep events in the middle of the floor slab cannot be differentiable with those close to the separation walls at the east end of the floor. For instance, in Fig. 10b, a high number of CLs are estimated for footstep events at location #20 for occupants O1 and O2 and event #18 for occupants O1, O2 and O5. The CLS of footstep event #20 for Occupant O5

does not include possible locations in the middle of the floor, and this results in two groups of possible locations at each side of the floor.

A high number of CLs may result from model simplifications including separation walls that are modelled using translational springs in the vertical direction (see Section 4.1). Taking the average stiffness value between freely supported and completely fixed, spring stiffnesses are conservative regarding the unknown connection types between walls and the floor slab. Also, adding heavy furniture or retrofitting the structure may significantly affect model predictions leading to inaccurate localization for long term applications. Thus, model calibration using a sensitivity analysis based on either footstep-induced floor vibrations or static loading could enhance the simulation of support stiffness. A multi-parametric sensitivity analysis to assess the variation of model predictions in the presence of structural and non-structural elements could improve robustness.

Additional sensors close to boundary conditions could be useful to decrease the number of CLs. Thus, a study of the sensor layout has potential for improving the precision of candidate locations. Moreover, further modal analyses of the floor slab close to the supports (walls and columns) is needed. Dividing the floor near the supports into zones of similar rigidities may enhance the determination of footstep-contact dynamics. Increasing knowledge of the behavior of the floor slab near supports has the potential to enhance the localization precision.

Footstep-contact dynamics are determined using vibration measurements from a single walking occupant. This implies that the localization is limited to one occupant at a time. More than one occupant walking simultaneously results in overlapping signals. Such responses require additional processing to separate signal contributions from each occupant to determine individual footstep-contact dynamics. Several methods, including blind source separation (BSS) [72] and equivariant adaptive separation (EAS) [73] methods have the potential to separate overlapping signals. Also, appropriate footstep-impact simulations to localize more than one occupant are under study for occupant detection and tracking. In addition, the evaluation of the accuracy of occupant localization using other model-based approaches is current work.

The zone-based occupant localization approach has the potential to be applied to any floor configuration since structure-specific behavior models are used to interpret vibration measurements. Application of the zone-based approach for localization can also be useful for multi-story-buildings presenting similar floor-slab configuration. This could lead to employing the same simulations for all floors for the identification of occupant locations. However, the dynamic response regarding footstep impacts may vary significantly between the lower and higher floors. Thus, a sensitivity analysis to study the dynamic variability in measured and simulated responses is needed for multi-story-building applications.

6. Conclusions

In this paper, a model-based data interpretation based on EDMF is carried out for accurate and precise identification of occupant locations. Traditional accommodation of model bias and systematic uncertainties leads methods that sacrifice precision for accuracy. Use footstep contact dynamics, as described in this paper, improves precision of occupant localization without loss of accuracy. This work has been evaluated on a full-scale case study. Precision of localization has been improved by 53 % with enhanced understanding of occupant characteristics compared with the traditional method. The conclusions are as follows:

- A model-based approach that includes structural behavior, systematic errors and model bias in the interpretation of vibration measurements leads to accurate localization of occupants.
- Defining levels of footstep-contact severity within zones of floor slab that display similar structural behavior improves precision of occupant localization without compromising accuracy.

- As indicated by others [43,45], the heel phase of walking gait pattern (impact and subsequent full-contact between heel and floor) is confirmed to be the most important factor for localization.

Funding

Declaration of Competing Interest

The authors declare that they have no known competing financial interests or personal relationships that could have appeared to influence the work reported in this paper.

Acknowledgments

References

[1] B. Song, H. Choi, H.S. Lee, Surveillance tracking system using passive infrared motion sensors in wireless sensor network, in: 2008 Int. Conf. Inf. Netw., 2008: pp. 1–5.

[2] W.P.L. Cully, S.L. Cotton, W.G. Scanlon, J.B. McQuiston, Localization algorithm performance in ultra low power active RFID based patient tracking, in: 2011 IEEE 22nd Int. Symp. Pers. Indoor Mob. Radio Commun., 2011: pp. 2158–2162.

[3] W.P.L. Cully, S.L. Cotton, W.G. Scanlon, Empirical performance of RSSI-based Monte Carlo localisation for active RFID patient tracking systems, Int. J. Wirel. Inf. Networks. 19 (2012) 173–184.

[4] G. Diraco, A. Leone, P. Siciliano, People occupancy detection and profiling with 3D depth sensors for building energy management, Energy Build. 92 (2015) 246–266.

[5] C.M. Stoppel, F. Leite, Integrating probabilistic methods for describing occupant presence with building energy simulation models, Energy Build. 68 (2014) 99–107.

[6] A.J. Newman, K.C. Daniel, D.P. Oulton, New insights into retail space and format planning from customer-tracking data, J. Retail. Consum. Serv. 9 (2002) 253–258.

[7] V. Uotila, P. Skogster, Space management in a DIY store analysing consumer shopping paths with data-tracking devices, Facilities 25 (2007) 363–374.

[8] A. Kamthe, L. Jiang, M. Dudys, A. Cerpa, Scopes: Smart cameras object position estimation system, in: Eur. Conf. Wirel. Sens. Networks, Cork, Ireland, 2009: pp. 279–295.

[9] A. Bamis, D. Lymberopoulos, T. Teixeira, A. Savvides, The BehaviorScope framework for enabling ambient assisted living, Pers. Ubiquitous Comput. 14 (2010) 473–487.

[10] G. Fierro, O. Rehmane, A. Krioukov, D. Culler, Zone-level occupancy counting with existing infrastructure, in: Proc. Fourth ACM Work. Embed. Sens. Syst. Energy-Efficiency Build., Toronto, Ontario, Canada, 2012: pp. 205–206.

[11] P. Lazik, N. Rajagopal, O. Shih, B. Sinopoli, A. Rowe, ALPS: A bluetooth and ultrasound platform for mapping and localization, in: Proc. 13th ACM Conf. Embed. Networked Sens. Syst., Seoul, South Korea, 2015: pp. 73–84.

[12] S. Narayana, R.V. Prasad, V.S. Rao, T. V Prabhakar, S.S. Kowshik, M.S. Iyer, PIR sensors: Characterization and novel localization technique, in: Proc. 14th Int. Conf. Inf. Process. Sens. Networks, Seattle, Washington, 2015: pp. 142–153.

[13] S. Budi, K. Hyoungseop, T.J. Kooi, I. Seiji, Real time tracking and identification of moving persons by using a camera in outdoor environment, (2009).

[14] Y. Zeng, P.H. Pathak, P. Mohapatra, WiWho: wifi-based person identification in smart spaces, in: Proc. 15th Int. Conf. Inf. Process. Sens. Networks, 2016: p. 4.

[15] P. Desai, N. Baine, K.S. Rattan, Indoor localization for global information service using acoustic wireless sensor network, in: Geospatial InfoFusion Syst. Solut. Def. Secur. Appl., 2011: p. 805304.

[16] X. Bian, G.D. Abowd, J.M. Rehg, Using sound source localization in a home environment, in: Int. Conf. Pervasive Comput., 2005: pp. 19–36.

[17] R. Serra, P. Di Croce, R. Peres, D. Knittel, Human step detection from a piezoelectric polymer floor sensor using normalization algorithms, in: SENSORS, 2014 IEEE, 2014: pp. 1169–1172.

[18] J. Yun, User identification using gait patterns on UbiFloorII, Sensors. 11 (2011) 2611–2639.

[19] R. Serra, D. Knittel, P. Di Croce, R. Peres, Activity recognition with smart polymer floor sensor: Application to human footstep recognition, IEEE Sens. J. 16 (2016) 5757–5775.

[20] D.T. Alpert, M. Allen, Acoustic gait recognition on a staircase, in: 2010 World Autom. Congr., 2010: pp. 1–6.

[21] J.T. Geiger, M. Kneißl, B.W. Schuller, G. Rigoll, Acoustic gait-based person identification using hidden Markov models, in: Proc. 2014 Work. Mapp. Personal. Trait. Chall. Work., 2014: pp. 25–30.

[22] A. Pakhomov, A. Sicignano, M. Sandy, E.T. Goldburt, Single-and three-axis geophone: footstep detection with bearing estimation, localization, and tracking, in: Unattended Gr. Sens. Technol. Appl. V, 2003: pp. 155–162.

[23] J. Schloemann, V.V.N.S. Malladi, A.G. Woolard, J.M. Hamilton, R.M. Buehrer, P.A. Tarazaga, Vibration event localization in an instrumented building, in: Exp. Tech. Rotating Mach. Acoust. Vol. 8, Springer, 2015: pp. 265–271.

[24] M. Lam, M. Mirshekari, S. Pan, P. Zhang, H.Y. Noh, Robust occupant detection through step-induced floor vibration by incorporating structural characteristics, in: Dyn. Coupled Struct. Vol. 4, Springer, 2016: pp. 357–367.

[25] M. Mirshekari, S. Pan, J. Fagert, E.M. Schooler, P. Zhang, H.Y. Noh, Occupant localization using footstep-induced structural vibration, Mech. Syst. Signal Process. 112 (2018) 77–97.

[26] J. Clemente, F. Li, M. Valero, W. Song, Smart seismic sensing for indoor fall detection, location and notification, IEEE J. Biomed. Heal. Informatics, 2019.

[27] I. Dokmanić, Listening to Distances and Hearing Shapes: Inverse Problems in Room Acoustics and Beyond, PhD Thesis EPFL. 6623 (2015), https://doi.org/10.5075/epfl-thesis-6623.

[28] J.D. Poston, R.M. Buehrer, P.A. Tarazaga, Indoor footstep localization from structural dynamics instrumentation, Mech. Syst. Signal Process. 88 (2017) 224–239.

[29] R. Bahroun, O. Michel, F. Frassati, M. Carmona, J.L. Lacoume, New algorithm for footstep localization using seismic sensors in an indoor environment, J. Sound Vib. 333 (2014) 1046–1066.

[30] S. Pan, M. Mirshekari, P. Zhang, H.Y. Noh, Occupant traffic estimation through structural vibration sensing, in: Sensors Smart Struct. Technol. Civil, Mech. Aerosp. Syst. 2016, Las Vegas, Nevada, USA, 2016: p. 980306.

[31] S. Drira, Y. Reuland, S.G.S. Pai, H.Y. Noh, I.F.C. Smith, Model-based occupant tracking using slab-vibration measurements, Front. Built Environ. 5 (2019) 63, https://doi.org/10.3389/fbuil.2019.00063.

[32] S. Drira, Y. Reuland, I.F.C. Smith, Model-based interpretation of floor vibrations for indoor occupant tracking, in: 26th Int. Work. Intell. Comput. Eng., Leuven Belgium, 2019.

[33] S. Drira, Y. Reuland, I.F.C. Smith, Occupant tracking using model-based data interpretation of structural vibrations, in: 9th Int. Conf. Struct. Heal. Monit. Intell. Infrastruct., St. Louis, MO, USA, 2019.

[34] A.G. Woolard, V.V.N.S. Malladi, S. Alajlouni, P.A. Tarazaga, Classification of event location using matched filters via on-floor accelerometers, in: Sensors Smart Struct. Technol. Civil, Mech. Aerosp. Syst. 2017, 2017: p. 101681A.

[35] S. Xu, L. Zhang, P. Zhang, H.Y. Noh, An information-theoretic approach for indirect train traffic monitoring using building vibration, Front. Built Environ. 3 (2017) 22.

[36] S.G.S. Pai, Y. Reuland, S. Drira, I.F.C. Smith, Is there a relationship between footstep-impact locations and measured signal characteristics? in: 1st ACM Int. Work. Device-Free Hum. Sens., New York, USA, 2019.

[37] S. Drira, S.G.S. Pai, I.F.C. Smith, Uncertainties in structural behavior for model-based occupant localization using floor vibrations, Front. Built Environ. (2021).

[38] Y. Reuland, S.G.S. Pai, S. Drira, I.F.C. Smith, Vibration-based occupant detection using a multiple-model approach, in: 35th Int. Conf. Struct. Dyn. Challenges Next Gener. Aerosp. Syst. (IMAC XXXV), Springer, Los Angeles, USA, 2017: pp. 49–56.

[39] J.-A. Goulet, I.F.C. Smith, Structural identification with systematic errors and unknown uncertainty dependencies, Comput. Struct. 128 (2013) 251–258.

[40] I.F.C. Smith, Studies of sensor data interpretation for asset management of the built environment, Front. Built Environ. 2 (2016) 8.

[41] R. Pasquier, I.F.C. Smith, Robust system identification and model predictions in the presence of systematic uncertainty, Adv. Eng. Informatics. 29 (2015) 1096–1109, https://doi.org/10.1016/j.aei.2015.07.007.

[42] S. Pan, N. Wang, Y. Qian, I. Velibeyoglu, H.Y. Noh, P. Zhang, Indoor person identification through footstep induced structural vibration, in: Proc. 16th Int. Work. Mob. Comput. Syst. Appl., Santa Fe, New Mexico, USA, 2015: pp. 81–86.

[43] V. Racic, A. Pavic, J.M.W. Brownjohn, Experimental identification and analytical modelling of human walking forces: Literature review, J. Sound Vib. 326 (2009) 1–49.

[44] J.R. Gage, P.A. Deluca, T.S. Renshaw, Gait analysis: principles and applications, JBJS. 77 (1995) 1607–1623.

[45] M.W. Whittle, Generation and attenuation of transient impulsive forces beneath the foot: a review, Gait Posture. 10 (1999) 264–275.

[46] M. Willford, C. Field, P. Young, Improved methodologies for the prediction of footfall-induced vibration, in, Build. Integr. Solut. (2006) 1–15.

[47] A.S. Mohammed, A. Pavic, V. Racic, Improved model for human induced vibrations of high-frequency floors, Eng. Struct. (2018) https://doi.org/10.1016/j.engstruct.2018.04.093.

[48] C.J. Middleton, J.M.W. Brownjohn, Response of high frequency floors: a literature review, Eng. Struct. 32 (2010) 337–352.

[49] V. Racic, J.M.W. Brownjohn, Stochastic model of near-periodic vertical loads due to humans walking, Adv. Eng. Informatics. (2011) https://doi.org/10.1016/j.aei.2010.07.004.

[50] A. Pavic, M.R. Willford, G. Appendix, Vibration serviceability of post-tensioned concrete floors, Post-Tensioned Concr Floors Des. Handb. (2005) 99–107.

[51] E.E. Ungar, J.A. Zapfe, J.D. Kemp, Predicting footfall-induced vibrations of floors, Sound Vib. 38 (2004) 16–22.

[52] T. Obata, Y. Miyamori, Identification of a human walking force model based on dynamic monitoring data from pedestrian bridges, Comput. Struct. 84 (2006) 541–548.

[53] A. Tongen, R.E. Wunderlich, Biomechanics of running and walking, Math. Sport. 43 (2010) 1–12.

[54] S. Drira, Y. Reuland, N.F.H. Olsen, S.G.S. Pai, I.F.C. Smith, Occupant-detection strategy using footstep-induced floor vibrations, in: Proc. 1st ACM Int. Work. Device-Free Hum. Sens., ACM, New York, NY, USA, 2019: pp. 31–34. https://doi.org/10.1145/3360773.3360881.

[55] A. Tarantola, Popper, Bayes and the inverse problem, Nat. Phys. 2 (2006) 492.

[56] K. Popper, The logic of scientific discovery, Hutchinson, London, 1959.

[57] R. Pasquier, L. D'Angelo, J.-A. Goulet, C. Acevedo, A. Nussbaumer, I.F.C. Smith, Measurement, data interpretation, and uncertainty propagation for fatigue assessments of structures, J. Bridg. Eng. 21 (2016) 4015087.

[58] Y. Reuland, P. Lestuzzi, I.F.C. Smith, Data-interpretation methodologies for non-linear earthquake response predictions of damaged structures, Front. Built Environ. 3 (2017) 43, https://doi.org/10.3389/fbuil.2017.00043.

[59] J.-A. Goulet, C. Michel, I.F.C. Smith, Hybrid probabilities and error-domain structural identification using ambient vibration monitoring, Mech. Syst. Signal Process. 37 (2013) 199–212.

[60] Z. Šidák, Rectangular confidence regions for the means of multivariate normal distributions, J. Am. Stat. Assoc. 62 (1967) 626–633, https://doi.org/10.1080/01621459.1967.10482935.

[61] M. Falbriard, Personal communication, Laboratory of Movement Analysis and Measurement, EPFL, Lausanne, 2019.

[62] M. Mirshekari, J. Fagert, A. Bonde, P. Zhang, H.Y. Noh, Human Gait Monitoring Using Footstep-Induced Floor Vibrations Across Different Structures, in: Proc. 2018 ACM Int. Jt. Conf. 2018 Int. Symp. Pervasive Ubiquitous Comput. Wearable Comput., 2018: pp. 1382–1391.

[63] T. Wang, O. Celik, F.N. Catbas, L.M. Zhang, A frequency and spatial domain decomposition method for operational strain modal analysis and its application, Eng. Struct. 114 (2016) 104–112.

[64] K. Kanazawa, K. Hirata, Parametric estimation of the cross-power spectral density, J. Sound Vib. 282 (2005) 1–35.

[65] A. Likas, N. Vlassis, J.J. Verbeek, The global k-means clustering algorithm, Pattern Recognit. 36 (2003) 451–461.

[66] J. Lin, L. Qu, Feature extraction based on Morlet wavelet and its application for mechanical fault diagnosis, J. Sound Vib. 234 (2000) 135–148.

[67] S.G.S. Pai, A. Nussbaumer, I.F.C. Smith, Comparing structural identification methodologies for fatigue life prediction of a highway bridge, Front. Built Environ. 3 (2018) 73.

[68] A.M. Apdl, Mechanical applications, Theory Reference (2010).

[69] M. Stein, Large sample properties of simulations using Latin hypercube sampling, Technometrics 29 (1987) 143–151.

[70] S. Chatterjee, A.S. Hadi, Sensitivity Analysis in Linear Regression, John Wiley & Sons, 2009.

[71] Y. Reuland, P. Lestuzzi, I.F.C. Smith, A model-based data-interpretation framework for post-earthquake building assessment with scarce measurement data, Soil Dyn. Earthq. Eng. 116 (2019) 253–263.

[72] S. Makino, S. Araki, R. Mukai, H. Sawada, Audio source separation based on independent component analysis. In: 2004 IEEE Int. Symp. Circuits Syst. (IEEE Cat. No. 04CH37512), 2004: pp. V–V.

[73] J.-F. Cardoso, B.H. Laheld, Equivariant adaptive source separation, IEEE Trans. Signal Process. 44 (1996) 3017–3030.